

WO: 2011-11043

Panel 35

GEOCREs No:
30M3-271-1

Report

to

Gartner Lee Limited

Effect of Excavation Process on the Glacial Sediments
at OWMC Landfill Site, West Lincoln

K.Y. Lo, R.K. Rowe and K.M. Lee

K.Y. LO INC.

July 1991

1. INTRODUCTION

In response to a request by Gartner Lee Limited (GLL) dated January 25, 1991 for a proposal to perform a study on the "Geotechnical Modelling to Characterize Deep Fractures in a Glacial Clay," a proposal was submitted on February 4, 1991. Following subsequent discussions between Gartner Lee Ltd. and K.Y. Lo Inc., a modified proposal was submitted on February 25, 1991 and work was authorized to proceed on April 1, 1991.

The scope of this investigation was to:

- (a) perform analyses of a 15 m deep excavation of a landfill in a 35 m thick layer of intact glacial clay, paying particular attention to the potential deformation and the development of tensile stresses and hence potential for inducing fractures at the bottom of the excavation;
- (b) examine the effect of "sequence of excavation and filling" of the landfill on the potential development of fractures; and
- (c) carry out a limited laboratory program so as to obtain a preliminary assessment of the undrained tensile strength of a glacial clay.

Information on soil properties and soil samples for testing were provided by Gartner Lee Ltd. (Gartner Lee Report GLL 88-573, 1989). Gartner Lee's results were assumed to be correct and were not checked.

The results of this preliminary study together with conclusions and recommendations are presented in this report.

2. SITE CONDITIONS

Gartner Lee's documentation (Report GLL 88-573, 1989) indicates that the OWMC's preferred site is underlain by approximately 35 m of overconsolidated glacial and glaciolacustrine silty clays, which in turn overlie a bedrock aquifer. It is understood that the proposed 1000 x 800 m landfill facility, which is to be constructed in stages at this site, will involve a 15 m deep excavation in these deposits (refer to section 2.2 for details). Shallow fractures up to 6 m deep have been reported throughout the site (GLL, 1988).

2.1 Geology

Based on the information provided by GLL, the overburden soil can be subdivided into four overburden geologic units of quaternary age as shown in Figure 1, namely (from surface to depth):

- (1) Upper Glaciolacustrine Unit (Unit 1): clayey silt to silty clay, occasional clast, commonly laminated, very stiff, medium plasticity;
- (2) Halton Unit (Unit 2): intermixed till and glaciolacustrine sediments, clayey silt, occasional clast, massive to poorly laminated, stiff to very stiff, low to medium plasticity;
- (3) Lower Glaciolacustrine Unit (Unit 3): glaciolacustrine sediments of clayey silt to silty clay, occasional clast, commonly laminated, stiff to very stiff, low plasticity; and

- (4) Lower Till (Unit 4): sand and silt, gravelly, massive, occasional sand inclusion, very dense to compact till.

Underlying these quaternary units is a dolostone bedrock of the Guelph and Lockport-Amabel formations.

2.2 The Proposed Landfill Concept

The following summarize our understanding of the landfill development concept. The proposed landfill will be constructed by the shallow entombment landfill concept, which involves the placement of all the treated solidified materials below the ground surface at depths between 5 and 15 m. Figures 2 and 3 illustrate the plan and cross-sections of the proposed landfill.

The proposed landfill is to be developed by a continuous area method. The landfill excavation and filling of the solidified material will be carried out in stages as shown in Figure 4. Basically, the landfill excavation will proceed forward in one direction with the filling operation following in behind. The maximum dimensions of the base of the excavation will be approximately 40 m x 160 m.

3. TESTING PROGRAM

On April 18, 1991, two 3 1/4" tube samples were obtained from GLL. It is understood that these piston samples were obtained from BH 85-2-1 and 85-15-1 at depths of 14.55 m - 16.07 m and 16.17 m - 17.69 m,

respectively. The depths of these samples were located near the bottom of the proposed landfill excavation and correspond to the Halton unit as defined in Figure 1. Detailed core descriptions of these two samples are given in Figure 5. Soil samples obtained from BH 85-2-1 were moist and generally in good condition. The sample obtained from BH 85-15-1, however, was partially dry and broken into pieces by drying cracks.

The following tests were performed on specimens trimmed from the tube samples at different depths:

- a) Four indirect tensile strength tests (Brazillian Tests) on samples at depths of 15.01 m, 15.61 m and 15.91 m from BH 85-2-1 and 16.32 from BH 85-15-1.
- b) Two Atterberg Limits tests on the samples of BH 85-2-1.
- c) One grain size distribution test on the sample of BH 85-2-1.

3.1 General Testing Procedures

The Atterberg Limits test and grain size distribution tests were performed according to the appropriate ASTM standards.

The four Brazillian tests were performed on soil samples trimmed to approximately 70 mm diameter and 100 mm long.

The test procedure followed was similar to the "Standard Test Method for Splitting Tensile Strength of Cylindrical Concrete Specimens," ASTM standard C496-86 (1987). The test involved the application of loading along the opposite sides of a cylindrical specimen in a compression machine until the load caused the specimen to split along the loaded

diameter.

The tensile strength σ_t (kPa) is calculated from the following equation:

$$\sigma_t = \frac{2P}{\pi DL} \quad (1)$$

where P = compression load at failure (kN),

D = diameter of the specimen (m), and

L = length of the specimen (m).

3.2 Test Results

The test results for Brazillian tests are summarized in Table 1. The test results for index tests are summarized in Table 2. Figure 6 gives the grain size distribution curve by hydrometer test from BH 85-2-1. From these results, the following observations can be made:

- (1) The results of tensile strength and natural water content for the three samples from BH 85-2-1 are very consistent with an average tensile strength of 69 kPa and water content of 19.3%.
- (2) The result of tensile strength for BH 85-15-1 is significantly higher than that of BH 85-2-1. The natural water content is much smaller than that of BH 85-2-1 and that reported by GLL. This discrepancy is caused by the partial drying of the piston sample and, therefore, results obtained from BH 85-15-1 will be discarded in later analyses.

- (3) The results of Atterberg Limit tests are very consistent and agree reasonably well with that reported by GLL. The averaged liquid limit (ω_L) is 32.4%, plastic limit (ω_p) is 16.5%, and natural water content (ω_n) is 19.3%.
- (4) The results of hydrometer analysis indicate that the soil sample from BH 85-2-1 consists of 55% silt and 45% clay size material (MIT classification) which is consistent with that reported by GLL.

4. SELECTION OF SOIL PARAMETERS FOR USE IN ANALYSES

The selection of soil parameters (i.e. drained vs undrained analysis) will be dependent on the rate of advancement of the excavation and filling as well as the time period between the completion and commencement of these two operations. It is important to note that the proposed landfilling operation is a dynamic process (i.e. the excavation face and filling working face move continuously across the site as shown in Figure 4). Based on the information provided by Gartner Lee Limited (GLL 88-573, 1989), the bottom of the excavation will be filled after approximately 5 months, and it will take approximately 19 months for an arbitrarily defined excavation "slot" to be completely filled. In light of these construction processes, only the "undrained" behaviour of the ground is considered in this study. Although it is recognized that some dissipation of induced pore pressure is likely to occur, this is considered to be a second order effect.

4.1 Fracture Mechanism

As working hypotheses prior to the preliminary study, it was assumed that fractures (in particular, the observed fracture systems located in glacial deposits in Southern Ontario) could be formed and modified by one or more of the following physical processes: i) desiccation, ii) rebound on unloading or stress release during erosion, and iii) propagation of reflection cracks from fracture systems in the underlying bedrock. The exact physical processes responsible for fracture initiation and growth in these glacial deposits, however, are poorly understood.

Based on the investigators' experience, it is considered that post-depositional processes of freeze-thaw action and desiccation (especially due to historically lower water levels) are the dominating fracturing mechanisms in the West Lincoln site. The penetration depths of these fracture systems are generally confined to near ground surface. It is understood that the possibility of structural discontinuity developed during the sedimentation process has been evaluated in an independent detailed site specific data and geomorphological assessment undertaken for Gartner Lee.

In this preliminary study, the effect of excavation of a 15 m deep landfill in a layer of 35 m thick intact glacial clay which is free of pre-existing fractures will be examined. Results from this analysis will indicate the likelihood of potential initiation of newly developed fracture systems as a result of landfill construction in intact deposits.

* FREEZE - THAW

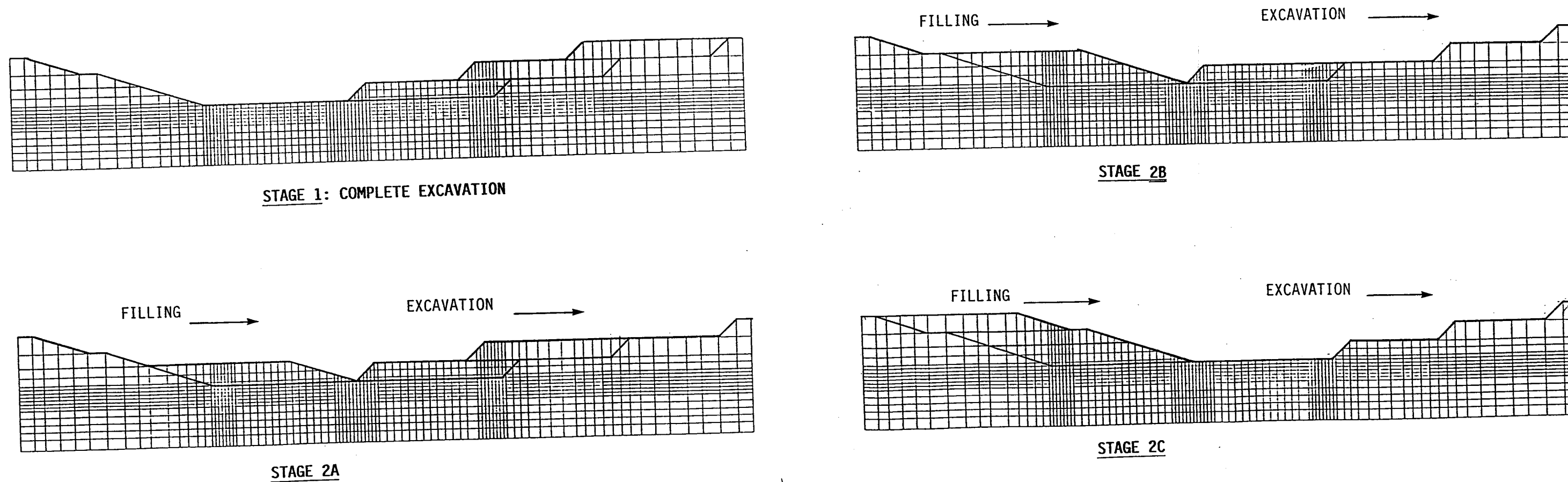
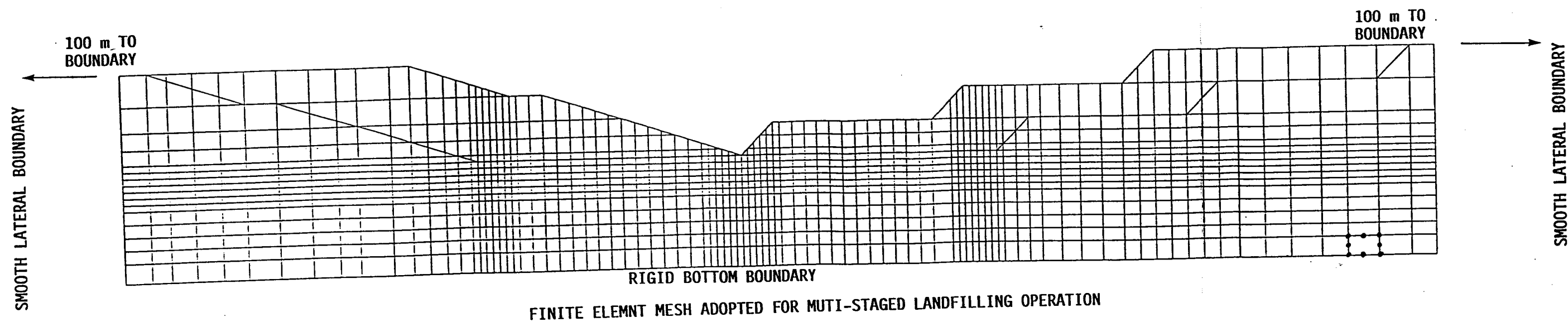


FIGURE 13 FINITE ELEMENT MESH AND SIMPLIFIED CONSTRUCTION SEQUENCE

4.2 Undrained Strength Profile

The undrained shear strength, c_u , values obtained from field vane tests (provided by GLL 88-573, 1989) are plotted in Figure 7. The c_u profile adopted for the present analyses is also shown in Figure 7. The strength profile adopted in the analysis decreases from 200 kPa at the ground surface (El. 185 m) to 100 kPa at El. 178 m (i.e. at a rate of 14.2 kPa/m) and remains constant at 100 kPa down to the Lower Till at El. 153 m. As noted by Lo (1965), the vane strength shown in Figure 7 approximately corresponds to the horizontal undrained strength c_{uh} of the undisturbed soil. The degree of strength anisotropy for the Halton (Unit 2) and Lower Glaciolacustrine Unit (Unit 3) had been examined by GLL, and they concluded that both units exhibit very little strength anisotropy.

4.3 Modulus Profile

An important input into the analyses is the magnitude and distribution of the undrained Young's modulus (E_u^*) with depth. It is known (Ng and Lo, 1985) that the unloading moduli (E_u^*), appropriate to excavation conditions, are typically substantially higher than the loading moduli (E_u).

Based on the results of consolidated undrained triaxial tests (CIU) on samples from BH 88-3-3 (obtained by Prof. R.M. Quigley - report to GLL on Feb. 2, 1989), the loading moduli at various initial confined pressures were estimated. The variation of the loading deformation moduli with the initial effective vertical pressure, σ_v' , is shown in Figure 8. For the

vertical stress range between 100 kPa to 600 kPa, the loading moduli increase from 16.8 MPa to 45 MPa. The loading modulus (E_u) at the elevation near the bottom of the landfill excavation is estimated to be approximately 17.5 MPa. The E_u/c_u ratio (under loading conditions) at this elevation is about 175.

The elastic moduli under "unloading" conditions can be estimated from anisotropically-consolidated undrained triaxial extension tests (CK_0UE). Since only the results of conventional CIU compression tests are available, the elastic modulus in extension (E_u^*) is estimated to be approximately 1.5-2.0 times the modulus in compression (i.e., $E_u^* \approx (1.5 \text{ to } 2.0) E_u$) as suggested by Ng and Lo (1980). For the purposes of this study, the lower factor of 1.5 was adopted.

Based on the results of CIU tests, and the assumption of $E_u^* \approx 1.5 E_u$, the distribution of modulus with depth may be developed as illustrated in Figure 9. It is assumed that a 7 m thick crust is present below ground surface and is underlain by a soil with a constant modulus value of 25 MPa down to the Lower Till layer (Unit 4). The modulus of the Lower Till is assumed to be 250 MPa.

4.4 In-Situ Stress State

A critical input into the analyses is the magnitude of in-situ stress state, in particular, the coefficient of earth pressure at rest (K_0). A knowledge of the in-situ state of stress is necessary for two reasons. Firstly, these stresses represent the original conditions onto

which the landfill construction imposes stress changes. These initial stresses will have an influence on the potential development of tensile stress and the overall engineering performance of the landfill facility. Secondly, nearly all engineering properties of soil are a function of the soil stresses, either directly or indirectly. Therefore, the stresses are needed to evaluate the soil properties.

In the present study, the initial vertical stress is assumed to be equal to the effective overburden stress in which $\sigma_{vo}' = \gamma'z$. The horizontal stress (σ_{ho}') is estimated using a coefficient of earth pressure at rest (K_o) for overconsolidated soils suggested by Mayne and Kulhawy (1982), viz.:

$$K_o = K_{o_{nc}} OCR^{\sin\phi'} \quad (2)$$

where OCR = overconsolidation ratio

$K_{o_{nc}}$ = coefficient of earth pressure at rest for normally consolidated soils

$$= 1 - \sin\phi' \text{ (Jaky, 1944)}$$

and ϕ' = angle of internal friction in terms of effective stresses for the normal consolidation state.

Information provided by GLL indicates that the OCR profile is highly non-uniform, being very high at the crust and decreasing to about 1.5 at the Lower Glaciolacustrine Unit (Unit 3). Adopting a possible range of OCR from 1.5 to 7, and assuming $\phi' = 27^\circ$, three limiting cases of K_o

condition will be examined:

Case i) Assuming $\phi' = 27^\circ$ and $OCR = 7$, gives $K_o = 1.3$. Hence,

$$\sigma_{ho}' = 1.3 \sigma_{vo}'$$

Case ii) Assuming $\phi' = 27^\circ$ and $OCR = 4$, gives $K_o = 1.0$. Hence,

$$\sigma_{ho}' = \sigma_{vo}'$$

Case iii) Assuming $\phi' = 27^\circ$ and $OCR = 1.5$, gives $K_o = 0.7$. Hence,

$$\sigma_{ho}' = 0.7 \sigma_{vo}'$$

It should be noted that the values of K_o obtained above are based on the empirical relationship derived from laboratory data.

It is expected that these three cases will likely demonstrate the effects of the state of in-situ stresses on the stresses and deformations of the excavation.

5. ANALYSIS OF PROPOSED LANDFILL

Two types of analysis were performed to examine the potential impact due to the removal of 15 m of the overburden clay for landfill construction:

- i) Three-Dimensional Finite Layer Analysis - The potential elastic ground deformations and tensile stress distribution can be estimated from this analysis. Results from this analysis can also be used to define a more "critical region" for detailed Finite Element analysis.

- ii) **Two-Dimensional Finite Element Analysis** - This analysis can be used to directly model the excavation and filling process on the glacial deposits. Results from this analysis can be used to assess the potential development of fractures beneath the excavation resulting from the removal of 15 m of the overburden clay for landfill construction.

From a synthesis of the results of these two approaches, an opinion may be formulated regarding the potential impact of the landfill construction on the physical characteristics of the underlying glacial deposits.

5.1 Three-Dimensional Finite Layer Analysis

An elastic three-dimensional finite layer analysis using the computer program FLANS (Rowe and Booker, 1982 - see Appendix I for a description of this program) was performed to determine the potential elastic deformations along the bottom of the proposed excavation level. This analysis takes into account the three-dimensional nature of unloading but does not explicitly model the excavation itself. Rather, in this approach, the landfill is represented by a number of "unloading areas" on a horizontal ground surface as shown in Figure 10. Landfill excavation is represented by seven rectangular areas of different "unloading pressures" to simulate different levels of excavation. By adopting the principle of superposition, the total vertical displacement along sections A-A and B-B (as shown in Figure 10) can be obtained. The assumed "unloading" geometry is considered to represent the excavation of the

first full "slot" of the proposed landfill. Although it is recognized that the actual geometry of the landfill configuration is not quite symmetrical in the direction of landfill advancement, the effect associated with the assumption of the symmetrical "unloading areas", as shown in Figure 10, is considered to be a second order effect in this case.

The vertical ground movement calculated from the 3D finite layer analysis is shown in Figures 11 and 12 for sections A-A and B-B, respectively. The maximum elastic ground heave is estimated to be about 10.5 cm, and occurs near the centre of excavation. As shown in Figure 12, vertical displacements between the width of excavation for section B-B are rather uniform, implying that the unloading within the excavation is approaching one-dimensional. The displacement profile for section A-A is more complex and suggests a more two-dimensional stress condition. The direction of cross-section A-A also coincides with the direction of the landfill construction processes. Therefore, this section is chosen for the detailed two-dimensional finite element analysis as described in the following section.

5.2 Two-Dimensional Finite Element Analysis

A two-dimensional plane strain finite element analysis was performed to indicate the effect the excavation would have on a transverse cross-section shown as section A-A on Figure 10 and illustrated on Figure 13. The proposed landfiling operation is a dynamic process whereby the

excavation face and filling face move continuously across the site. In an attempt to capture the essential features of this operation, the following four stages of a simplified construction sequence (see Figure 13) were analyzed. (Note: This staging scheme is for computational purposes only.)

- Stage 1 - The landfill is assumed to be excavated quickly to a depth of 15 m. The maximum width at the bottom of excavation is 40 m. This stage of excavation is considered to represent the first full "slot" of excavation of landfill in the glacial deposits.
- Stage 2A - Placing a 5 m thick solidified waste lift to cover the bottom of excavation, together with the excavation of 5 m of glacial deposit from the ground surface.
- Stage 2B - Placing an additional 5 m of solidified waste material, and excavation of another 5 m of glacial deposit.
- Stage 2C - Placing a 5 m thick compacted earth cover and final excavation of 5 m of glacial deposit to give a new slot with a total depth of 15 m. At the end of stage 2C, the landfill is advanced forward by 40 m compared with the end of stage 1. Any subsequent landfilling operation can be simulated by repeating application of stages 2A to 2C.

The analyses were performed using the elasto-plastic finite element program AFENA (see Appendix II for details). The finite element mesh adopted in the analysis is shown in Figure 13, and consisted of 1680

eight-noded isoparametric elements with 10526 degrees of freedom. Because of the nonsymmetric nature of the excavation, it was necessary to model the soil to a considerable distance on both sides of the landfill as indicated in Figure 13. The analysis was performed for the undrained strength profile and modulus profile shown in Figures 7 and 9, respectively. The other properties of the soil are given in Table 3. The unit weight of the solidified waste material is assumed to be 12.5 kN/m^3 (i.e. the average of values of 12 kN/m^3 to 13 kN/m^3 provided by GLL). The unit weight of the compacted cover material is assumed to be 19 kN/m^3 .

5.2.1 Predicted Ground Deformations

The deformations along the bottom of the excavation calculated from this analysis are summarized in Table 4 and Figures 15, 16 and 17 for the cases of $K_o = 0.7$, $K_o = 1.0$ and $K_o = 1.3$, respectively (see Figure 14 for the location of reference points and reference of horizontal distances). For the case of $K_o = 0.7$, the predicted maximum bottom heave at the end of stage 1 and stage 2 are 13 cm and 12 cm, respectively. These agree quite well with the value of 10.5 cm calculated from elastic finite layer analysis. However, the predicted maximum bottom heave for the cases of $K_o = 1.0$ and $K_o = 1.3$ increase to 35.6 cm and 65.2 cm, respectively.

This significant increase in bottom heave under higher K_o conditions can be explained by the development of plastic zones as shown in Figures 18, 19 and 20 for the cases of $K_o = 0.7$, 1.0 and 1.3, respectively. It can be seen that the plastic zone for $K_o = 0.7$ is limited, and confined to

limited depths below the bottom of excavation. The predicted ground deformations therefore are largely elastic (and hence the good agreement with the 3D elastic analysis). At the end of the second stage of excavation, all the soil becomes elastic. On the other hand, plastic zones were predicted to be of significant extent for both the cases of $K_0 = 1.0$ and 1.3 . The onset of plasticity for the latter two cases may induce significant amounts of permanent plastic deformation, as manifest in Figures 16 and 17. At the end of the second stage excavation, the amounts of plasticity are generally reduced, and become insignificant for $K_0 = 1.0$.

Results from these analyses seem to indicate that the first full "slot" of excavation in the ground (as simulated by stage 1 excavation) is the most critical case. The magnitude of bottom heave and the amount of plasticity are highly dependent upon the assumed K_0 condition. This relationship can best be illustrated by a plot of bottom heave versus percentage of excavation of the ground as shown in Figure 21. (Excavation of the landfill was simulated by first deducing the equivalent nodal forces that would be acting around the excavated boundary prior to excavation, and then removing these nodal forces to create a stress-free surface. The percentage of excavation is defined as the proportion of the total nodal force removed to simulate the progressive excavation.) For the cases of $K_0 = 1.0$ and $K_0 = 1.3$, deformations increase rapidly as the excavation exceeds about 75% and 40%, respectively. This increase in rate of displacement is due to an increase in the extent of the plastic zone.

On the other hand, the ground response remains largely elastic throughout the excavation for the case of $K_0 = 0.7$.

The subsequent stages of landfilling operations as simulated by stages 2A, 2B and 2C appear to produce a less "critical" effect as compared with the stage 1 simulation. The reasons for this behaviour can be explained by the "stress path" concept as discussed in the following section.

5.2.3 Predicted Stress Changes

Stress paths calculated by the finite element analyses are shown in Figures 22, 23 and 24 for K_0 conditions of 0.7, 1.0 and 1.3, respectively. In each of these plots, three locations were considered as shown in Figure 14. Location 640 is approximately 1 m below the bottom of excavation, location 632 is approximately 5 m above the bedrock and along the centre-line of excavation, while location 1315 is at the edge of the first stage of excavation and approximately 20 m below the original ground surface.

Along the centreline of the excavation (i.e. locations 632 and 640), the induced stress changes are very close to that for one-dimensional unloading conditions (i.e., the total reduction of horizontal stresses is small and the total reduction of vertical stresses is almost equivalent to the weight of excavated overburden soil of 300 kPa). This one-dimensional unloading condition will cause the stress path to travel in a sub-vertical direction until it intersects with the failure envelope. Subsequent filling and excavation activities as simulated by stages 2A,

2B and 2C will cause the stress paths to travel away from the failure envelope (i.e. the so-called "elastic unloading"), therefore reducing the total amount of plasticity.

The stress changes at location 1315 (i.e. near the edge of the excavation) are quite different to that along the centreline of excavation. Stress changes at this location are more complicated and two-dimensional in nature, but remain elastic for all the cases examined.

For the cases considered in this preliminary study, all the horizontal stresses beneath the excavation are in compression and therefore prohibiting the development of new fractures at the floor of the excavation. Tensile stresses are only predicted to occur near the crest of the side slopes. The locations of these tensile stresses are illustrated in Figures 18, 19 and 20. Maximum tensile stresses were predicted to locate at a distance approximately 40 m from the crest of the side slopes. The maximum horizontal stress profiles after stage 1 excavation are shown in Figures 25, 26 and 27 for various K_0 . The depth of tensile stress distribution predicted by these analyses ranges from 5 m to 7 m below the original ground surface. A higher value of K_0 tends to increase the magnitude of tensile stress and the depth of tensile zone.

It should be noted that, in the present study, the ground is assumed to be intact and free of pre-existing fractures. The presence of deep-seated fracture systems may cause redistribution and/or propagation of tensile stresses to a larger depth.

5.3 Discussion of Results

The deformations and stress changes due to the excavation of a 15 m deep landfill have been calculated using both a 2D cross-sectional finite element analysis and a 3D elastic finite layer analysis. Comparison of the results under elastic conditions (i.e., for $K_0 = 0.7$) from the two analyses indicates reasonable agreement. Based on the geometry and the results of these analyses, it is considered that a 2D finite element analysis is reasonable for the preliminary study described in this report.

Results predicted by the two-dimensional finite element analysis indicate that the ground deformations induced by the proposed landfill are highly dependent on the in-situ stress state of the ground and, in particular, the coefficient of earth pressure at rest, K_0 . In the present analysis, three K_0 conditions have been examined. This range of K_0 values was adopted based on the empirical relationship derived from laboratory data, and it is expected that these cases will bracket the likely range of in-situ stress state of the ground. However, it should be noted that the actual K_0 profile in the ground is probably non-uniform with higher values near the crust and lower values with depth. However, detailed information describing the distribution of K_0 with depth was not available for the present analysis. This is considered to be the major uncertainty in the analysis and a detailed in-situ field testing and laboratory testing program would be required to better define the in-situ stress state and the K_0 distribution profile with depth and hence improve the

accuracy of the analysis. Further investigation into the effect of assumed non-uniform K_0 profile on the excavation of the landfill would also be warranted but would not negate the need for actual field data in a complete study of the problem.

6. CONCLUSIONS AND RECOMMENDATIONS

A preliminary investigation has been performed to evaluate the effects of a 15 m deep excavation in a layer of 35 m thick intact glacial clay. Three-dimensional elastic finite layer analysis and two-dimensional elasto-plastic finite element analysis were performed to identify the potential impact of the landfill excavation. Based on the results of this study, the following conclusions may be drawn:

- (a) Provided the ground is intact and free of deep-seated fractures, tensile stresses are only predicted to occur near the crest of the side slopes and these do not penetrate deeper than about 7 m below the ground surface and, therefore, will not induce any vertical fractures below the bottom of the proposed excavation for the geometry and soil parameters considered.
- (b) The predicted ground deformations induced by the proposed landfill construction are highly dependent upon the in-situ stress state of the ground (in particular, the coefficient of earth pressure at rest, K_0).

- (c) If a favourable in-situ stress state is present so that the deformations of the ground remain largely elastic, the predicted maximum heave at the bottom of excavation is about 12 cm.
- (d) If the in-situ stress state is less favourable (i.e., $K_0 > 1.0$), large bottom heave is anticipated and the stability of the proposed landfilling scheme should be carefully evaluated.
- (e) The excavation of the first full "slot" of landfill is considered to be the most critical case.

It should be noted that the results of this investigation and subsequent conclusions are based on limited information. In particular, the distribution of lateral earth pressure at rest (K_0) and undrained modulus have been assumed and these may have a significant influence on the calculated results. The accuracy of prediction from the model can be no better than the accuracy of input data. It was intended that the study described herein, provide an indication of potential effect and identify critical parameters. However, it should be emphasized that it is evident from this study that the prediction of the actual expected response of the proposed landfill can not be undertaken with the available data which were obtained for other purposes other than this study. It is recommended that future investigations focus on:

- (a) better defining the in-situ stress state and K_0 distribution profile with depth by means of in-situ field testing and laboratory testing;
- (b) evaluating the undrained modulus of the soil based on the results of appropriate laboratory tests;
- (c) refining the analysis using the results from (a) and (b) above.

7. REFERENCES

1. Gartner Lee Limited (1988). Site Assessment - Phase 4B: Geology, Hydrogeology and Geotechnics Reports, Addendum No. 1.
2. Gartner Lee Limited (1989). Site Assessment - Phase 4B: Geology, Hydrogeology and Geotechnics Reports, Addendum No. 2, Geotechnical Assessment of the Conceptual Landfill Design, prepared for Ontario Waste Management Corporation, GLL 88-573.
3. Jaky, J. (1944). The coefficient of earth pressure at rest. Magyar Mernok es Epiteaz Egylet Kozlonye.
4. Lo, K.Y. (1965). Stability of slopes in anisotropic soils. ASCE Journal of the Soil Mechanics and Foundations Division, 91(SM4): 85-106.
5. Mayne, P.W. and Kulhawy, F.H. (1982). K_0 -OCR relationships in soil. ASCE Journal of the Geotechnical Engineering Division, 108(GT6): 851-872.
6. Ng, R.M.C. and Lo, K.Y. (1985). The measurements of soil parameters relevant to tunnelling in clays. Canadian Geotechnical Journal, 22: 375-391.
7. Rowe, R.K. and Booker, J.R. (1982). Finite layer analysis of non-homogeneous soils. ASCE Journal of the Geotechnical Engineering Division, 108: 115-132.

TABLE 1 RESULTS OF SPLITTING TENSILE STRENGTH TESTS ON STIFF CLAY

Borehole No.	Sa. No.	Depth	Diameter	Height	Unit Weight	Failure Load	Tensile Strength			Water Content
							(kPa)	(psi)	(psf)	(%)
85-2-1	BR/2-1-1									
85-2-1	BR/2-1-2	15.01	69.9	99.8	2.08	777	71.0	10.3	1480	19.3
85-2-1	BR/2-1-3	15.61	69.9	106.4	2.15	751	64.3	9.3	1340	19.2
85-2-1	BR/2-1-4	15.91	69.9	108.0	1.99	843	71.2	10.3	1490	19.5
85-15-1	BR/15-1-1	16.32	69.9	105.3	2.13	1929	167.0	24.2	3490	16.7

TABLE 2 RESULTS OF ATTERBERG LIMITS (BH 85-2-1)

Sample No.	Depth (m)	Liquid Limit ω_L (%)	Plastic Limit ω_p (%)	Natural Moisture Content, ω_o (%)
2	15.01	32.0	16.8	19.3
3	15.61	32.8	16.3	19.2

TABLE 3 SOIL PARAMETERS ADOPTED IN THE ANALYSIS

Soil Parameter	Upper Glaciolacustrine Unit	Halton Unit	Lower Glaciolacustrine Unit
Unit Weight (kN/m^3)	19.0	20.0	19.0
Poisson's Ratio, ν	0.49	0.49	0.49
Undrained Strength, c_u (kPa)	Crust 200-100 kPa, then 100 kPa constant (see Figure 7)		
Undrained Modulus, E_u (MPa)	See Figure 9		
K_o	0.7 - 1.0 - 1.3		
Tensile Strength	69	69	69

TABLE 4 PREDICTED BOTTOM HEAVE FROM 2D FINITE ELEMENT ANALYSIS

K_0	Bottom Heave at the End of First Cycle of Excavation (cm)	Bottom Heave at the End of Second Cycle of Excavation and Filling (cm)
0.7	13.0	12.0
1.0	35.6	10.0
1.3	65.2	8.0

WEST

LOOKING NORTH

EAST

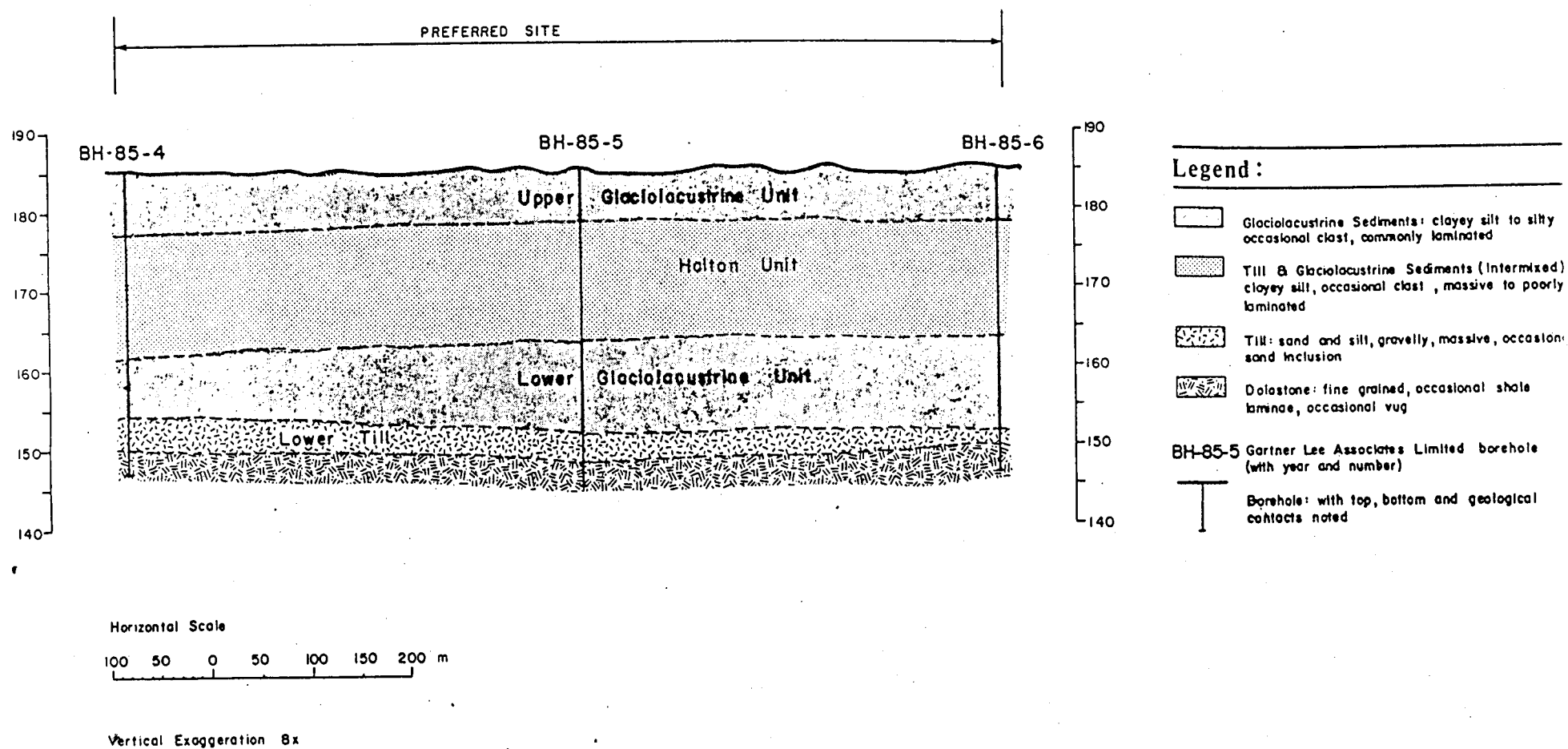


FIGURE 1 GEOLOGIC UNITS (after GLL, 1989)

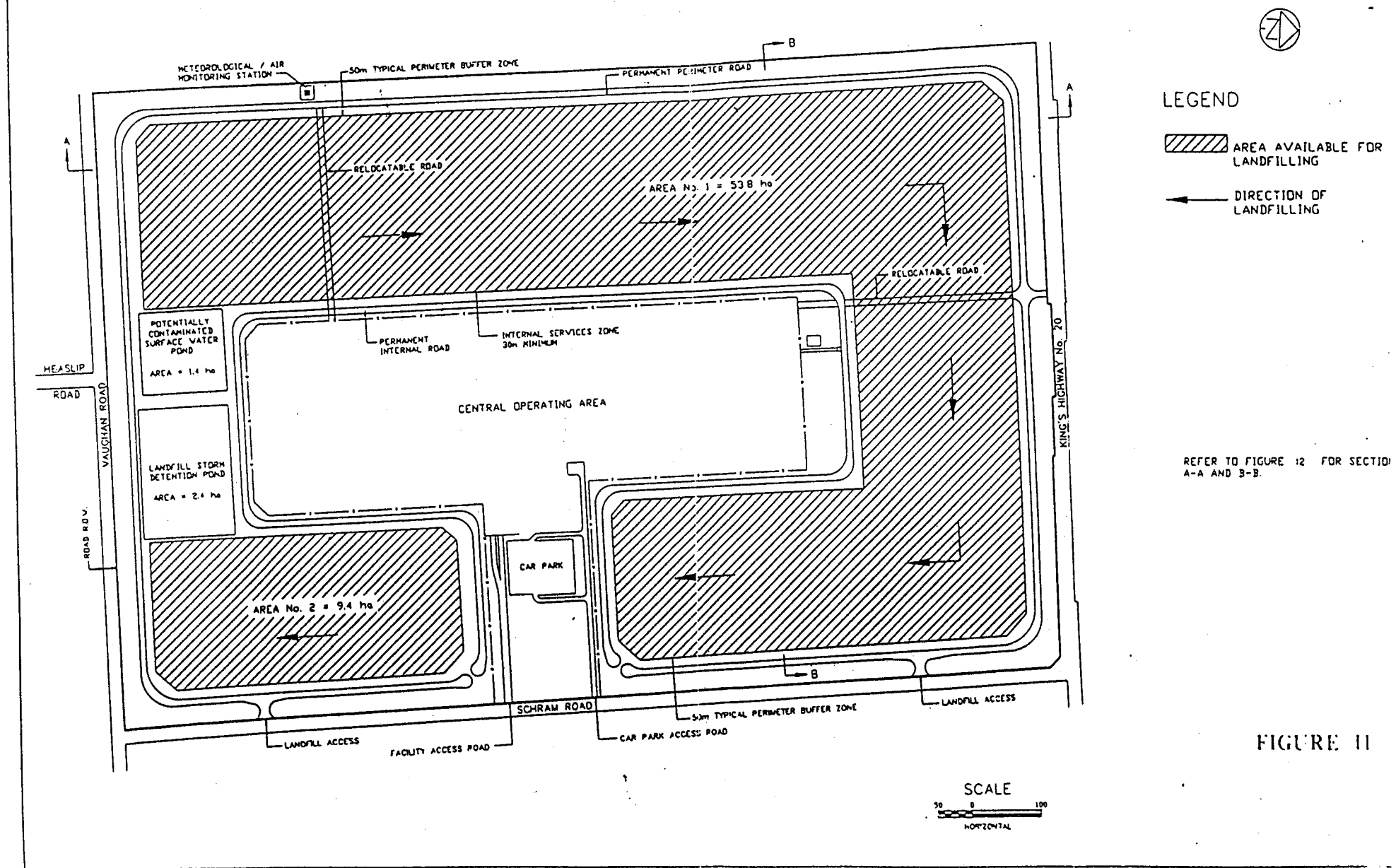


FIGURE 2 PLAN VIEW OF THE PROPOSED LANDFILL (after GLL, 1989)

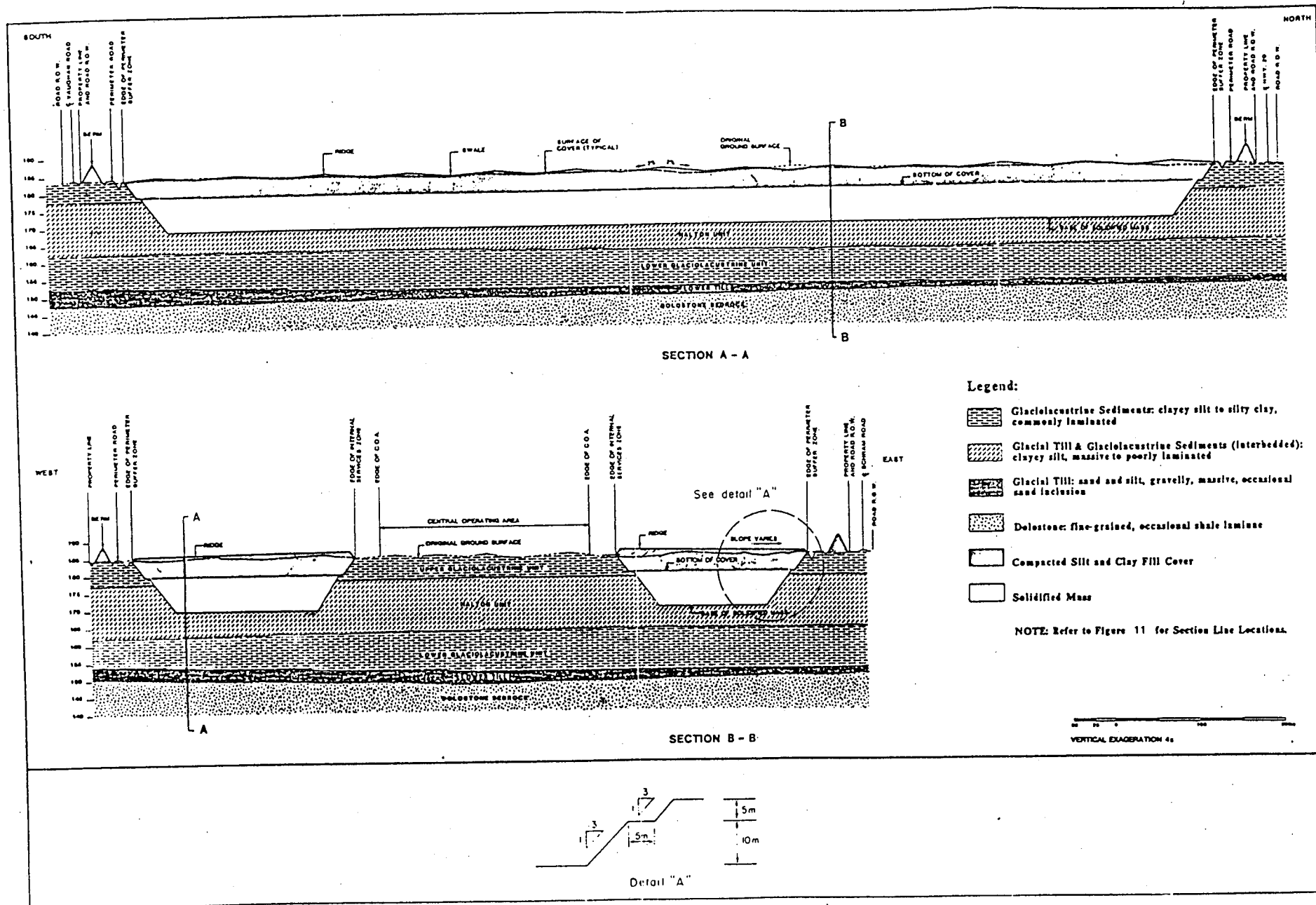


FIGURE 3 CROSS-SECTIONS OF THE PROPOSED LANDFILL (after GLL, 1989)

BH 85-2-1

1" GRAVEL

1½" GRAVEL

FINE SAND/
SILT POCKET

1½" GRAVEL

Sa. No.
Br/2-1-4

Depth
(m)

14.55

Sa. No.
Br/2-1-2

Sa. No.
Br/2-1-3

15.07

T
C
R

S
C
R

R
Q
D

Core Description

MASSIVE
REDDISH-BROWN
CLAYEY SILT,
VERY STIFF WITH
SCATTERED SAND
AND GRAVEL (gravel
with size upto 1½")
OCCASIONAL FINE
SAND OR SILT
INCLUSION

BH 85-15-1

DRYING CRACK

SILT LAYER

1" GRAVEL

SILT POCKET

DRYING CRACK

SILT LAYER
WITH SCATTERED
GRAVEL

DRYING CRACK

SILT LAYER

GRAVEL POCKET

Depth
(m)

16.17

Sa. No.
Br/15-1-1

17.69

T
C
R

S
C
R

R
Q
D

Core Description

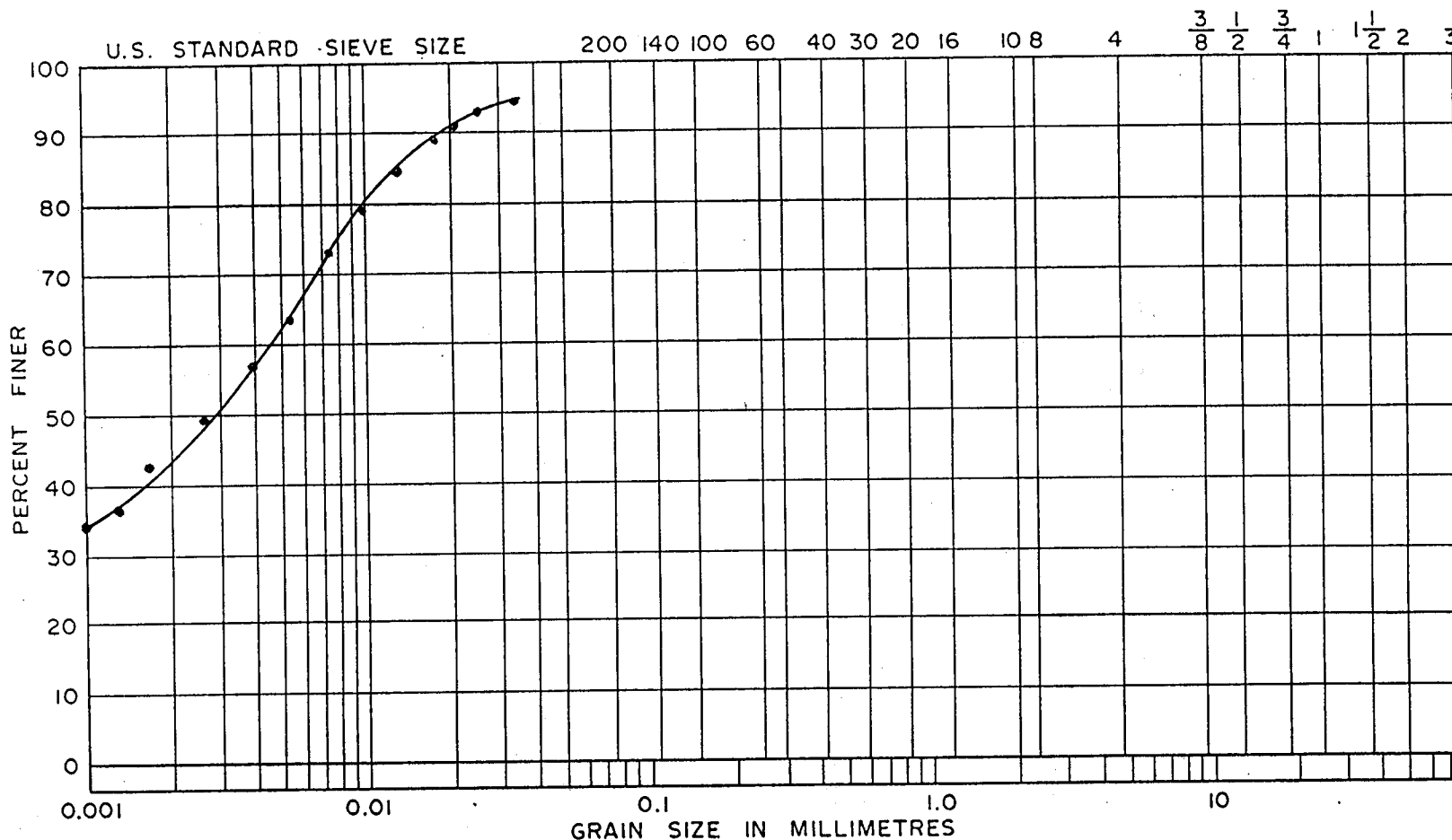
PARTIALLY DRY
REDDISH-BROWN
CLAYEY SILT WITH
SILT/FINE SAND
LAYERS, VERY STIFF
WITH SCATTERED
GRAVEL OF SIZE UP TO
1". DRYING CRACKS
OBSERVED ALONG SILT
LAYERS. CLAY LAYERS
ARE MASSIVE.

FIGURE 5 CORE DESCRIPTION FOR BH 85-2-1 AND BH 85-15-1

GRAIN SIZE DISTRIBUTION

THE UNIVERSITY OF WESTERN ONTARIO
GEOTECHNICAL LABORATORY

DATE 28 JUNE 1991
LOCATION West Lincoln OWMC Site
BOREHOLE NO. BH 85-2-1
SAMPLE NO. #1
DEPTH 14.55m - 16.07m
TESTED BY KML



M.I.T. CLASSIFICATION SYSTEM

CLAY	SILT	FINE	MEDIUM	COARSE	FINE	MEDIUM	COARSE
				SAND			
					GRAVEL		

UNIFIED CLASSIFICATION SYSTEM

UNITED CLASSIFICATION SYSTEM					
CLAY AND SILT	FINE	MEDIUM	COARSE	FINE	COARSE
	SAND			GRAVEL	

FIGURE 6 GRAIN SIZE DISTRIBUTION CURVE DETERMINED BY HYDROMETER ANALYSIS

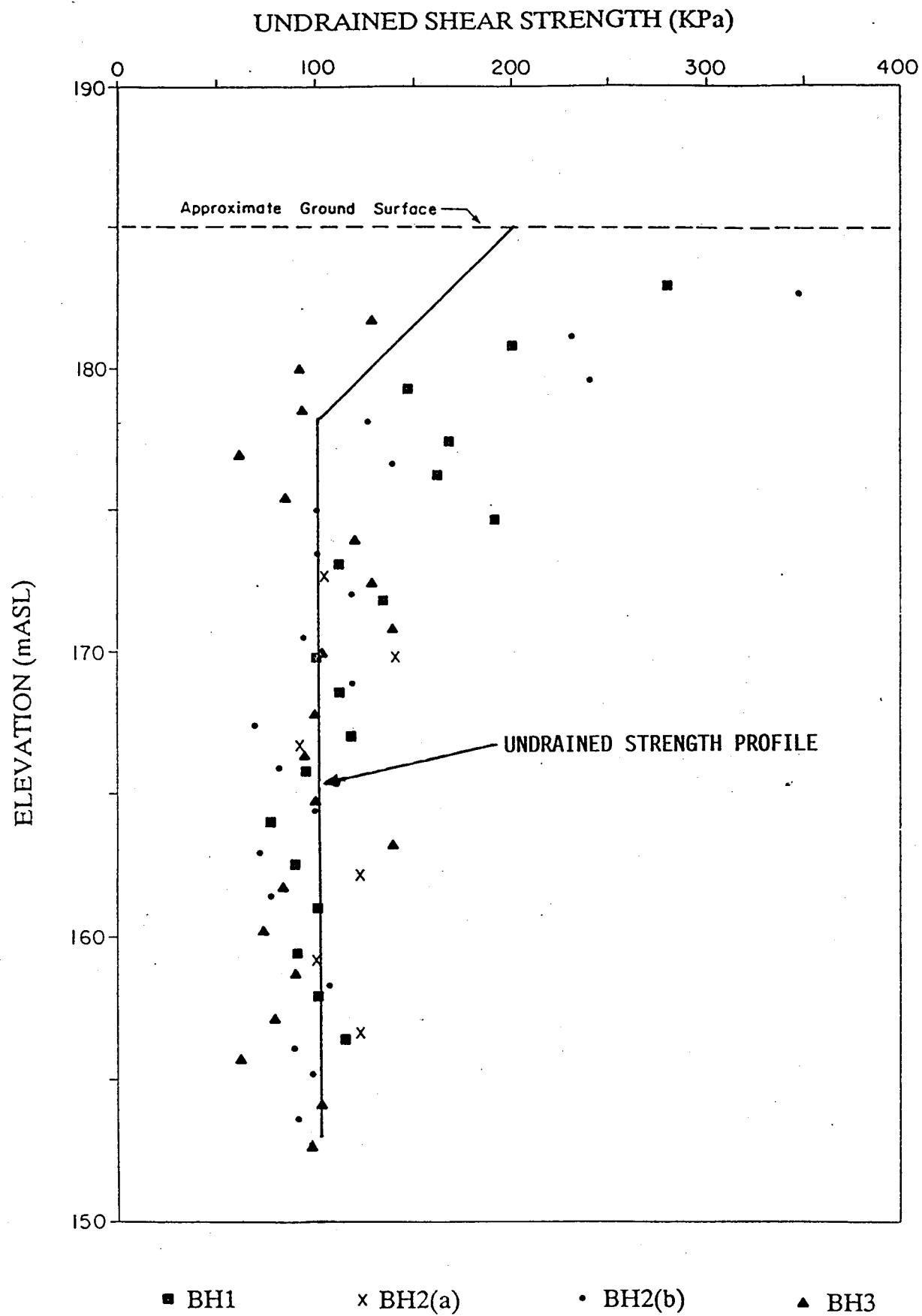


FIGURE 7 FIELD VANE STRENGTH AND ADOPTED c_u PROFILE

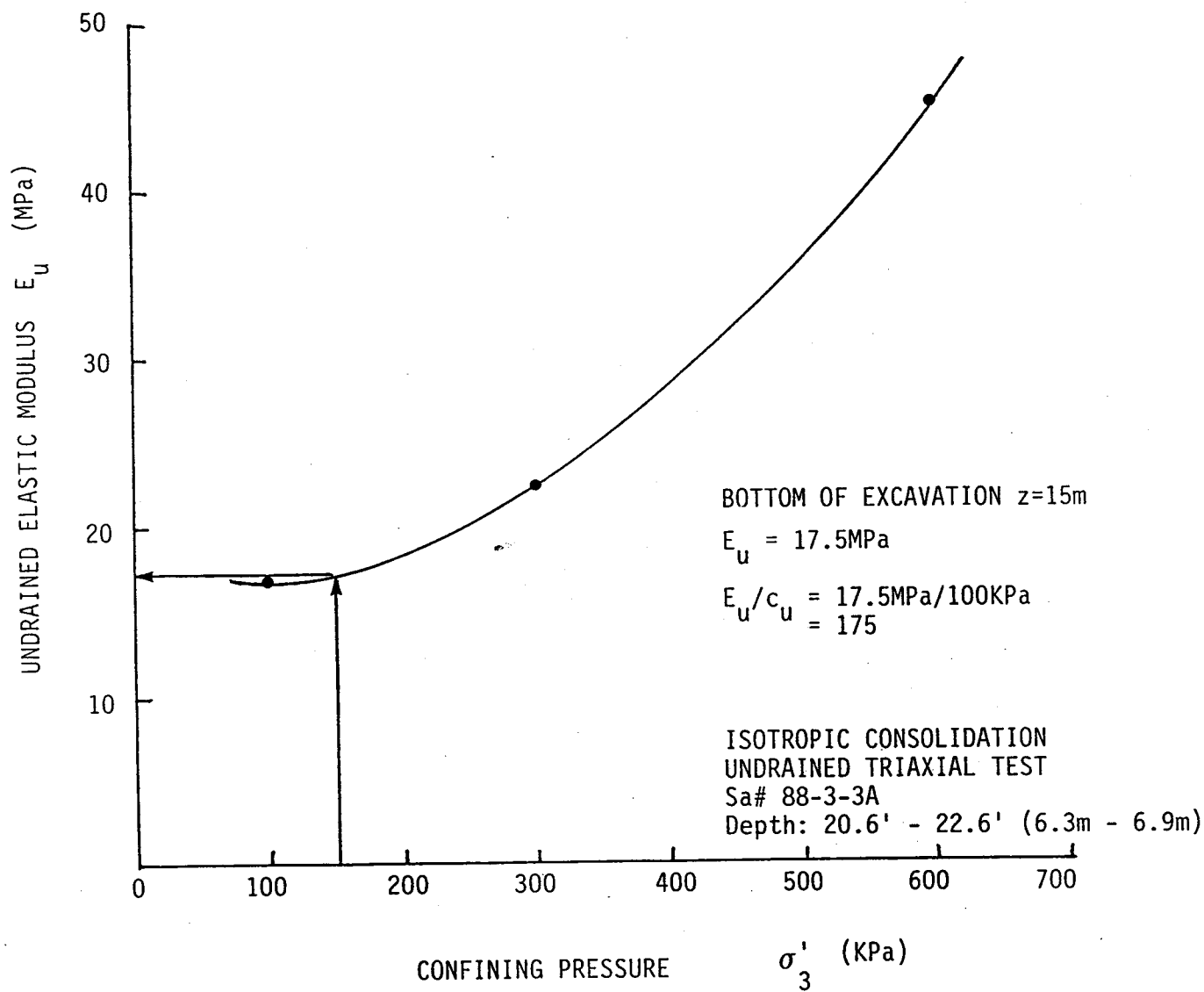


FIGURE 8 CONFINING PRESSURE VS. UNDRAINED MODULUS OBTAINED BY CIU TESTS

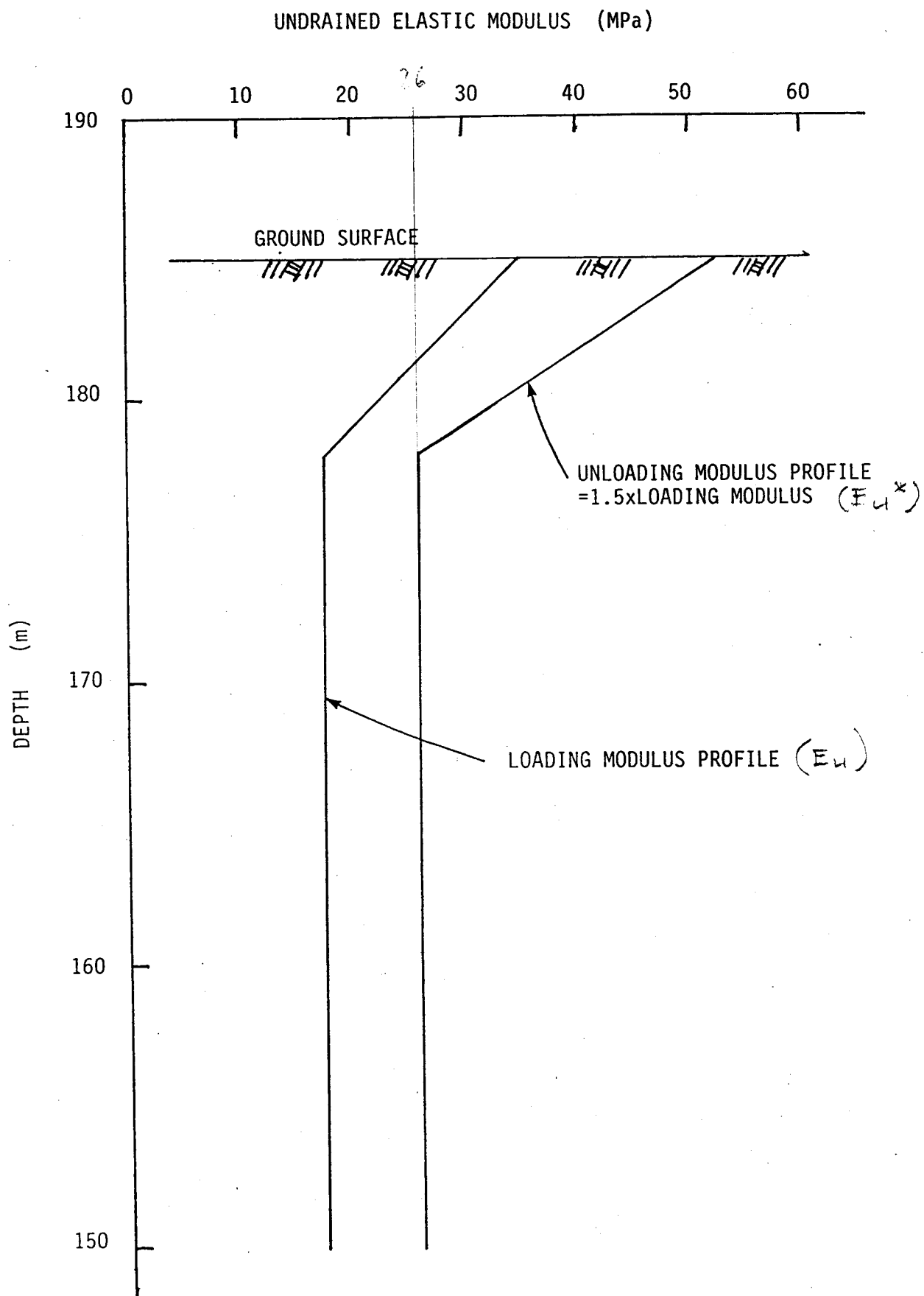


FIGURE 9 LOADING AND UNLOADING MODULUS PROFILES ADOPTED IN THE ANALYSIS

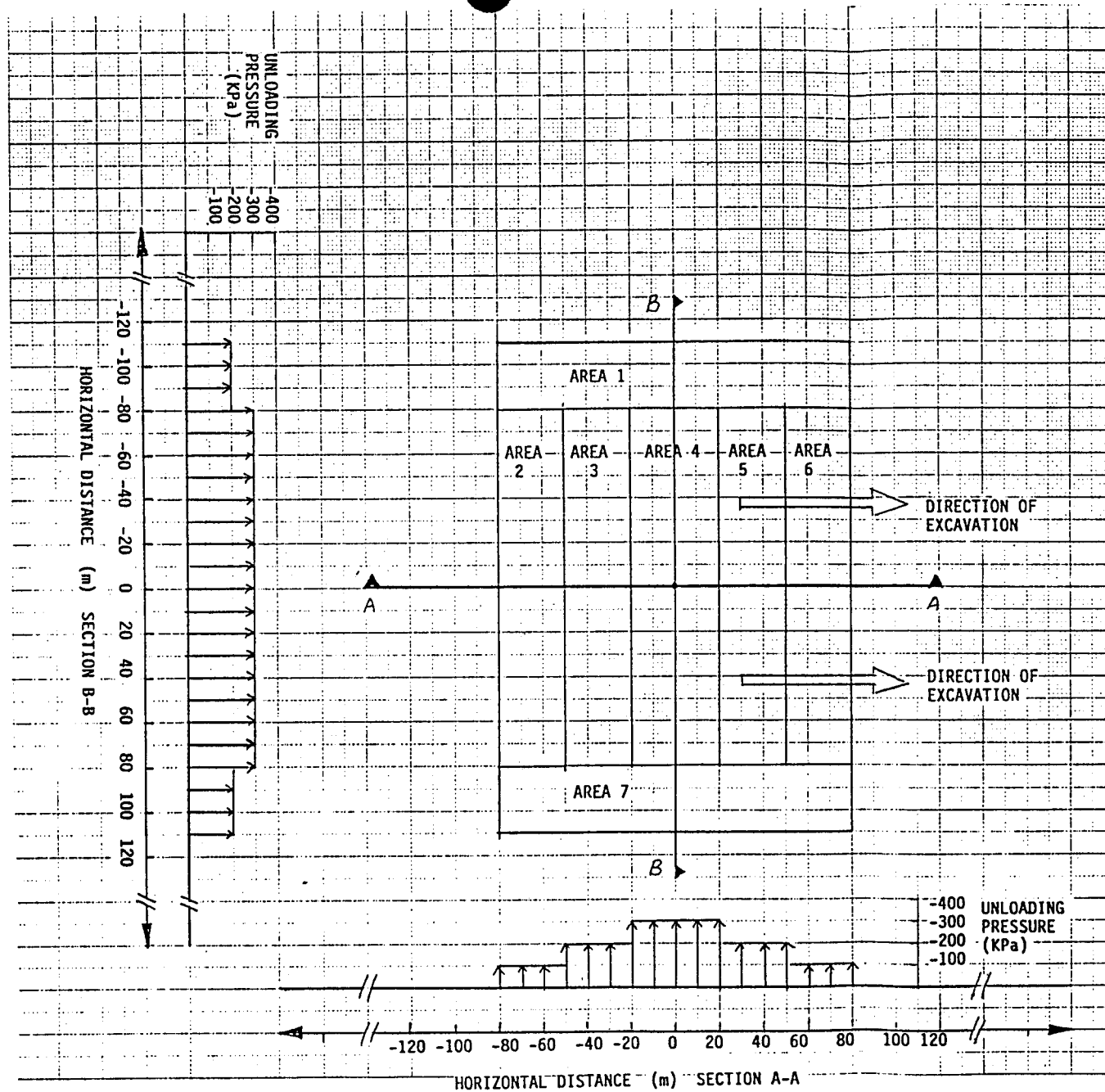


FIGURE 10 APPROXIMATE AREA TECHNIQUE TO MODEL THE PROPOSED LANDFILL FOR 3D FINITE LAYER ANALYSIS

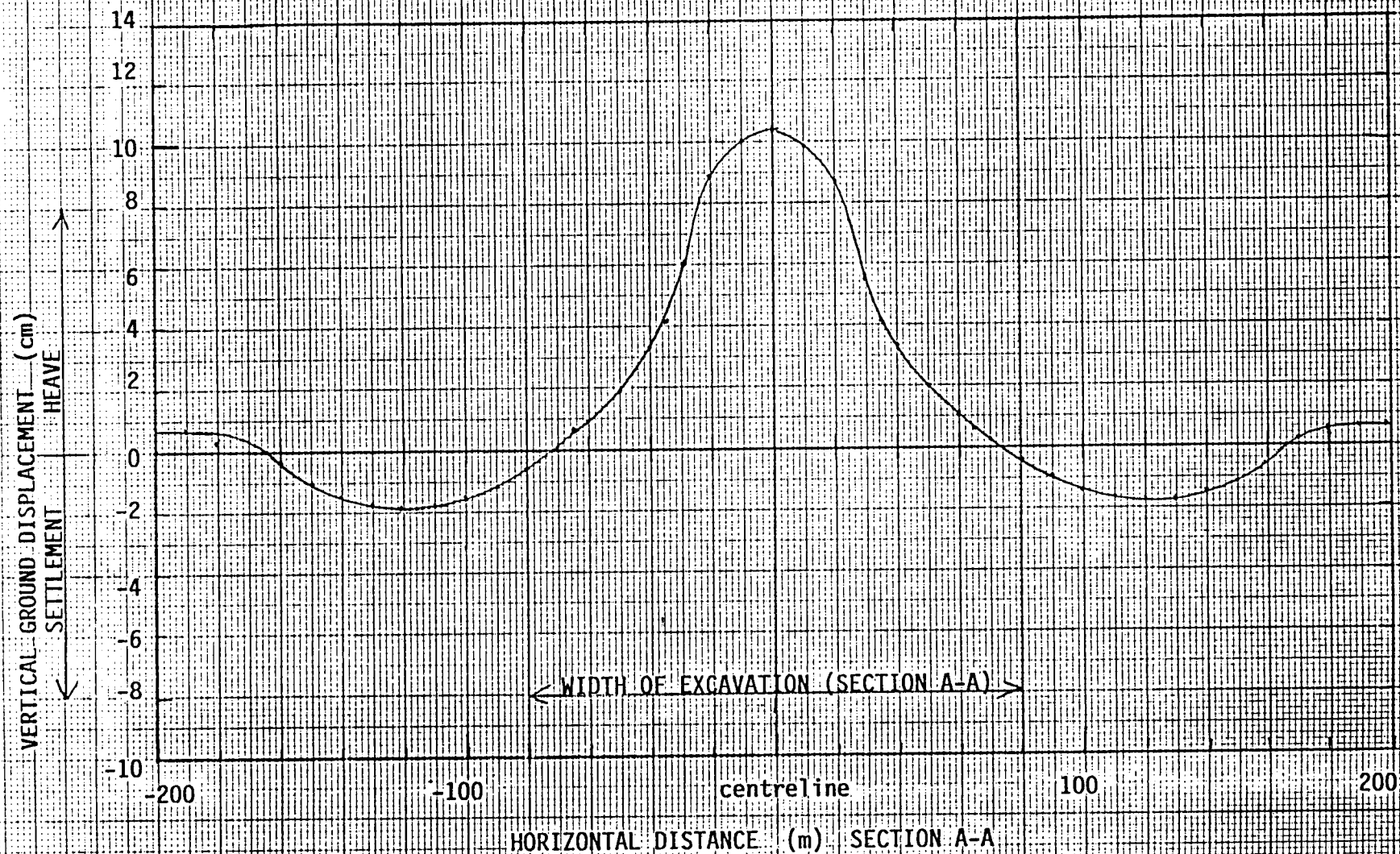
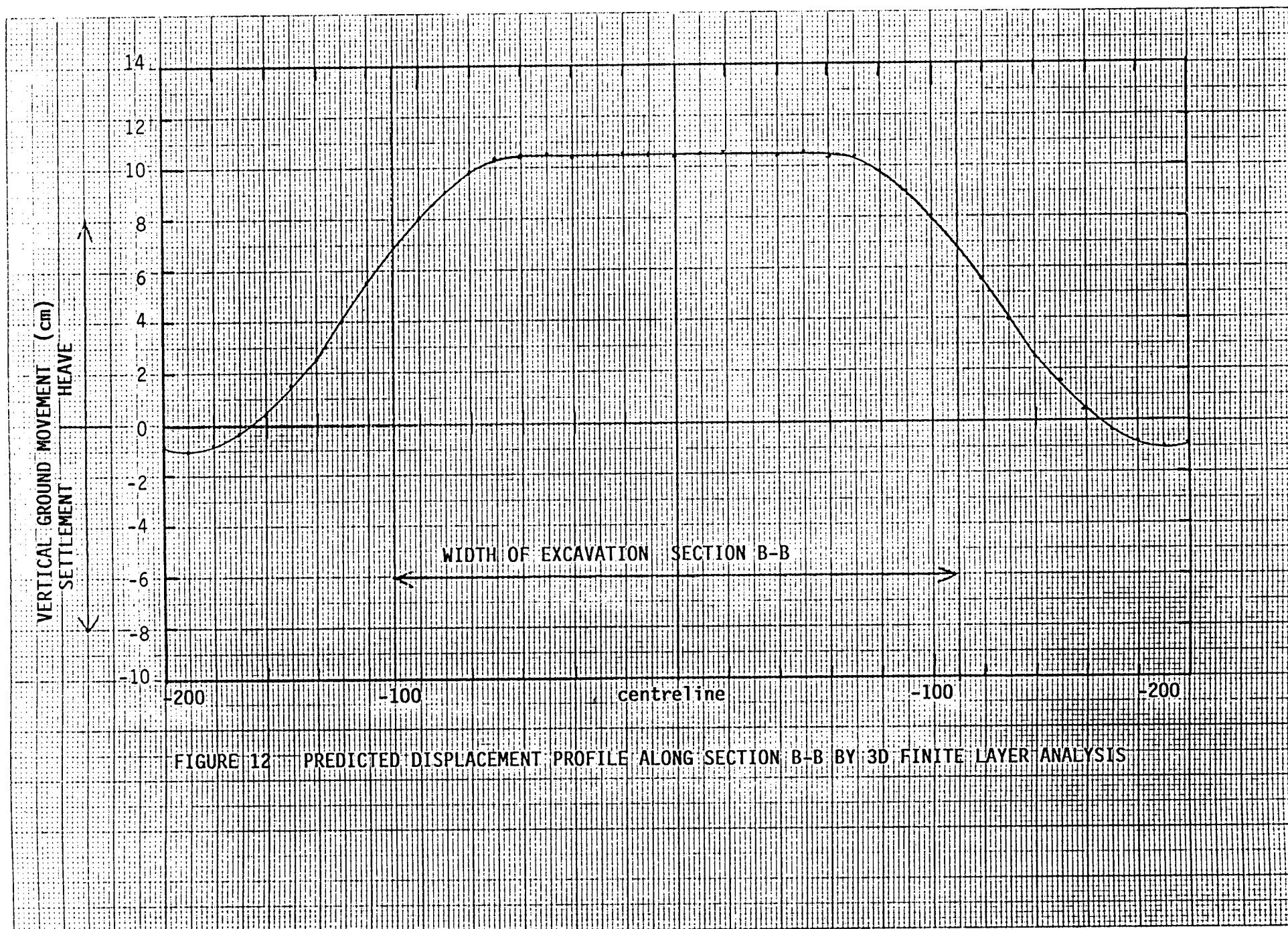


FIGURE 11 PREDICTED DISPLACEMENT PROFILE ALONG SECTION A-A BY 3D FINITE LAYER ANALYSIS



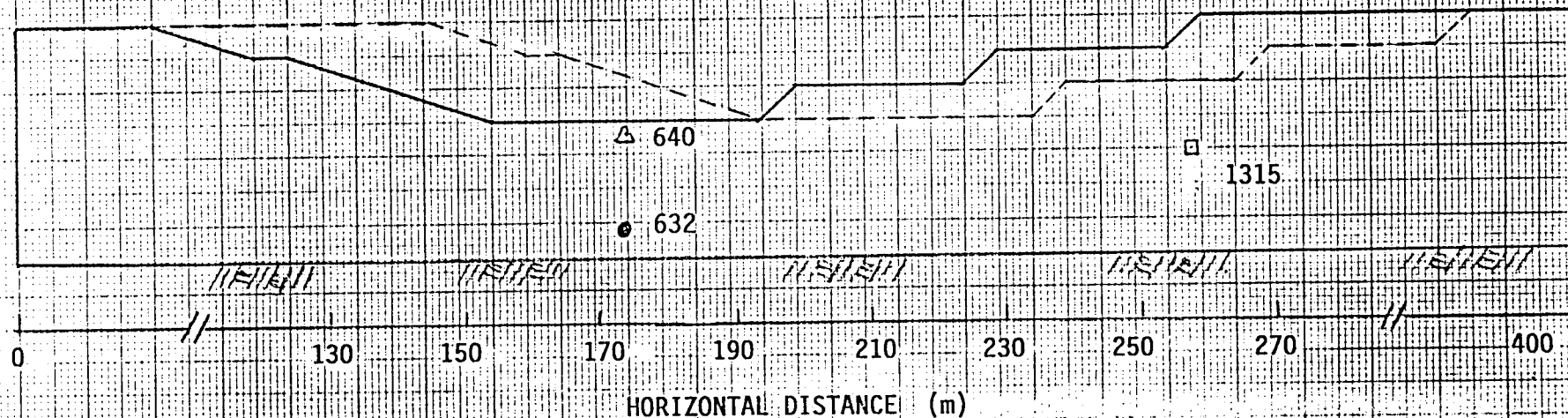


FIGURE 14 REFERENCE LOCATIONS

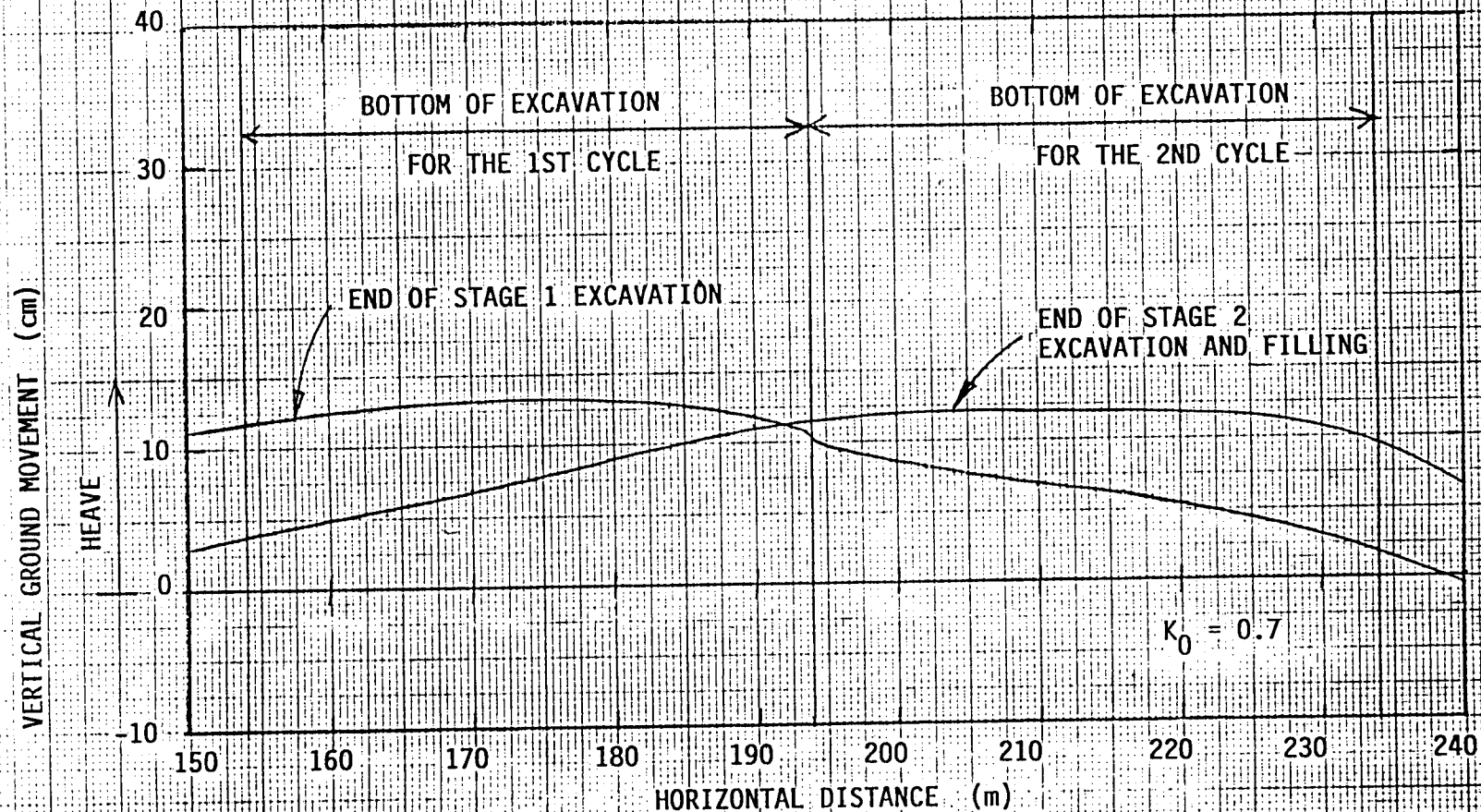


FIGURE 15 PREDICTED GROUND MOVEMENT ALONG BOTTOM OF EXCAVATION ($K_0 = 0.7$)

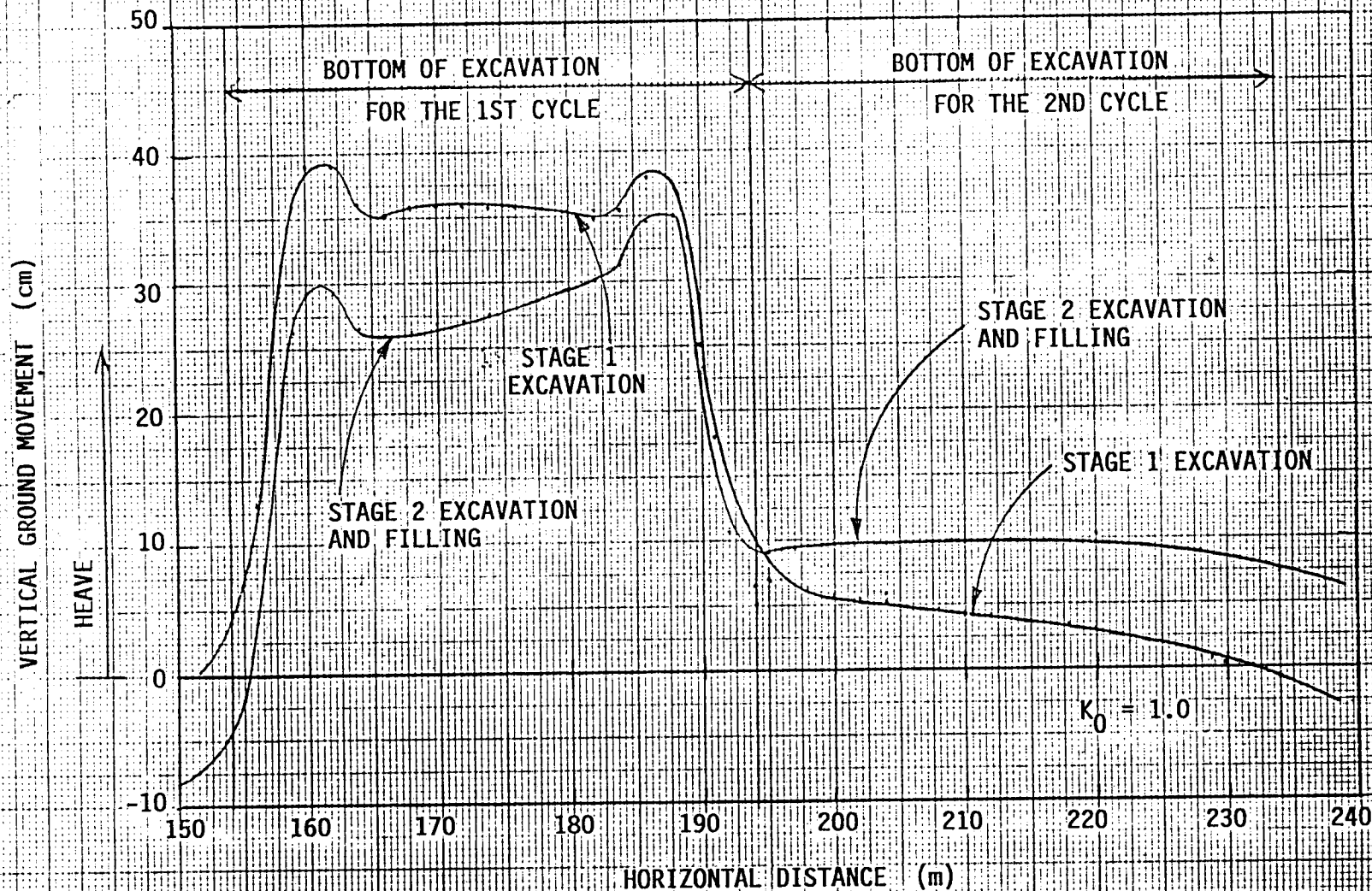


FIGURE 16 PREDICTED GROUND MOVEMENT ALONG BOTTOM OF EXCAVATION ($K_0 = 1.0$)

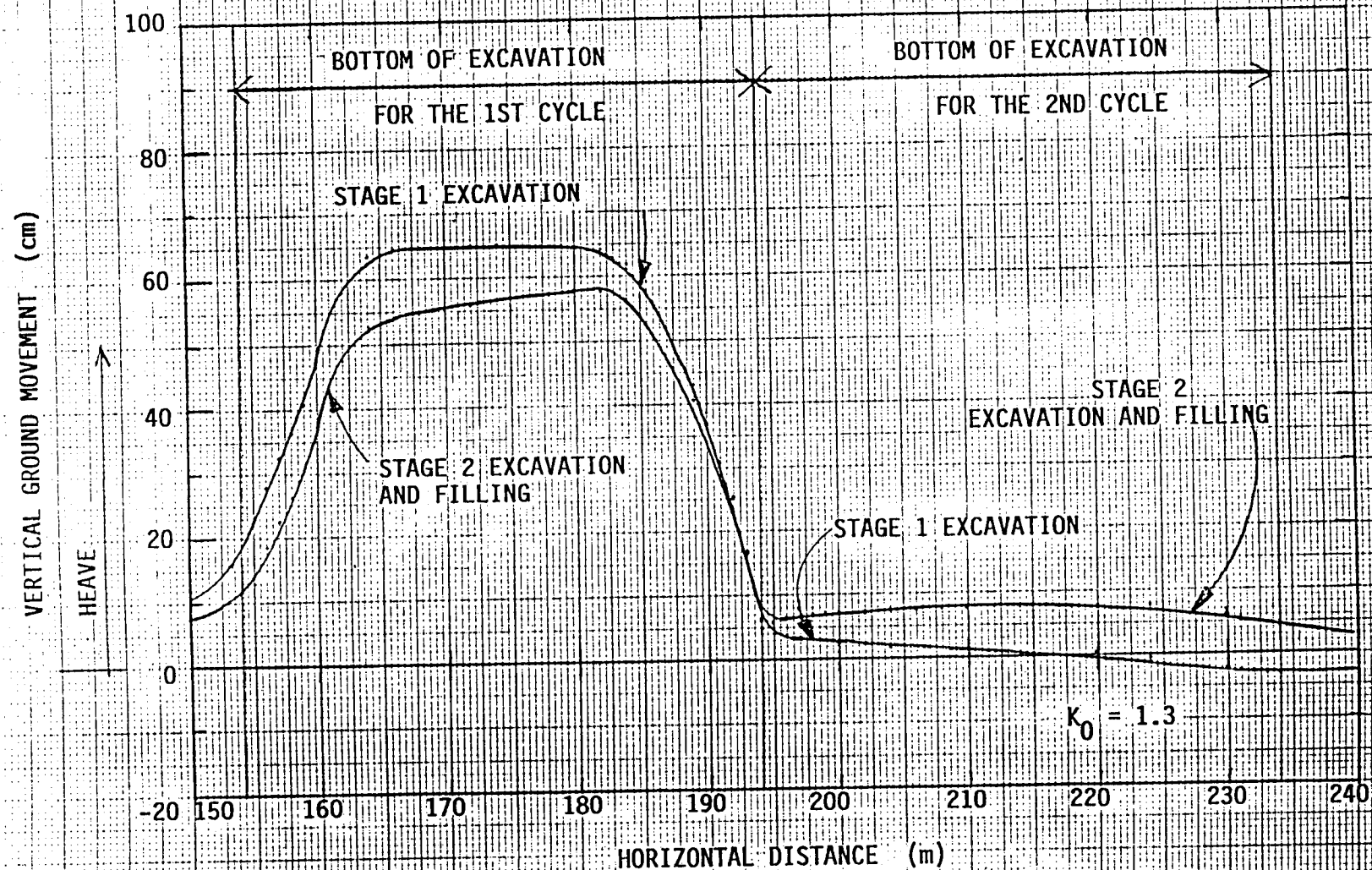


FIGURE 17 PREDICTED GROUND MOVEMENT ALONG BOTTOM OF EXCAVATION ($K_0 = 1.3$)

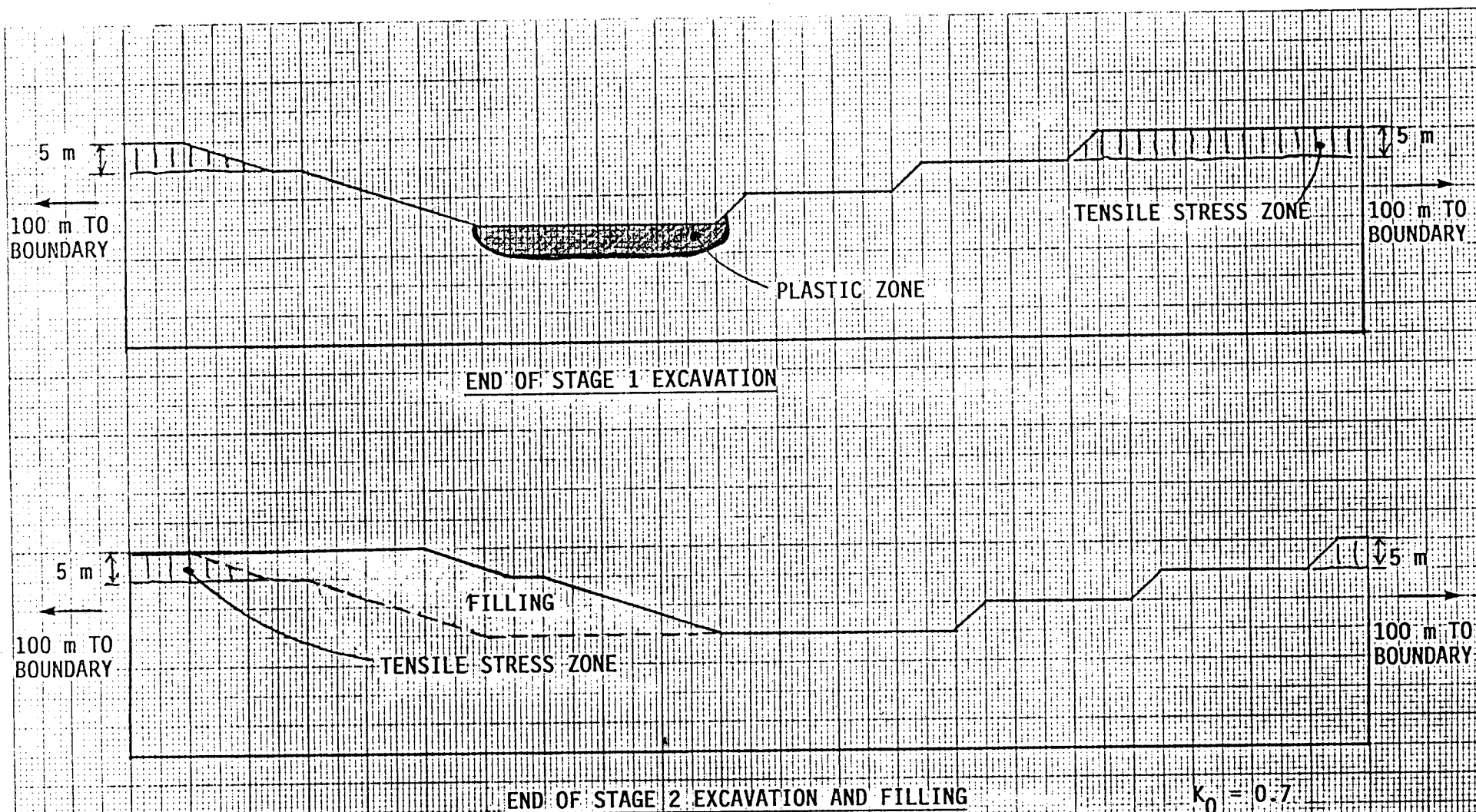
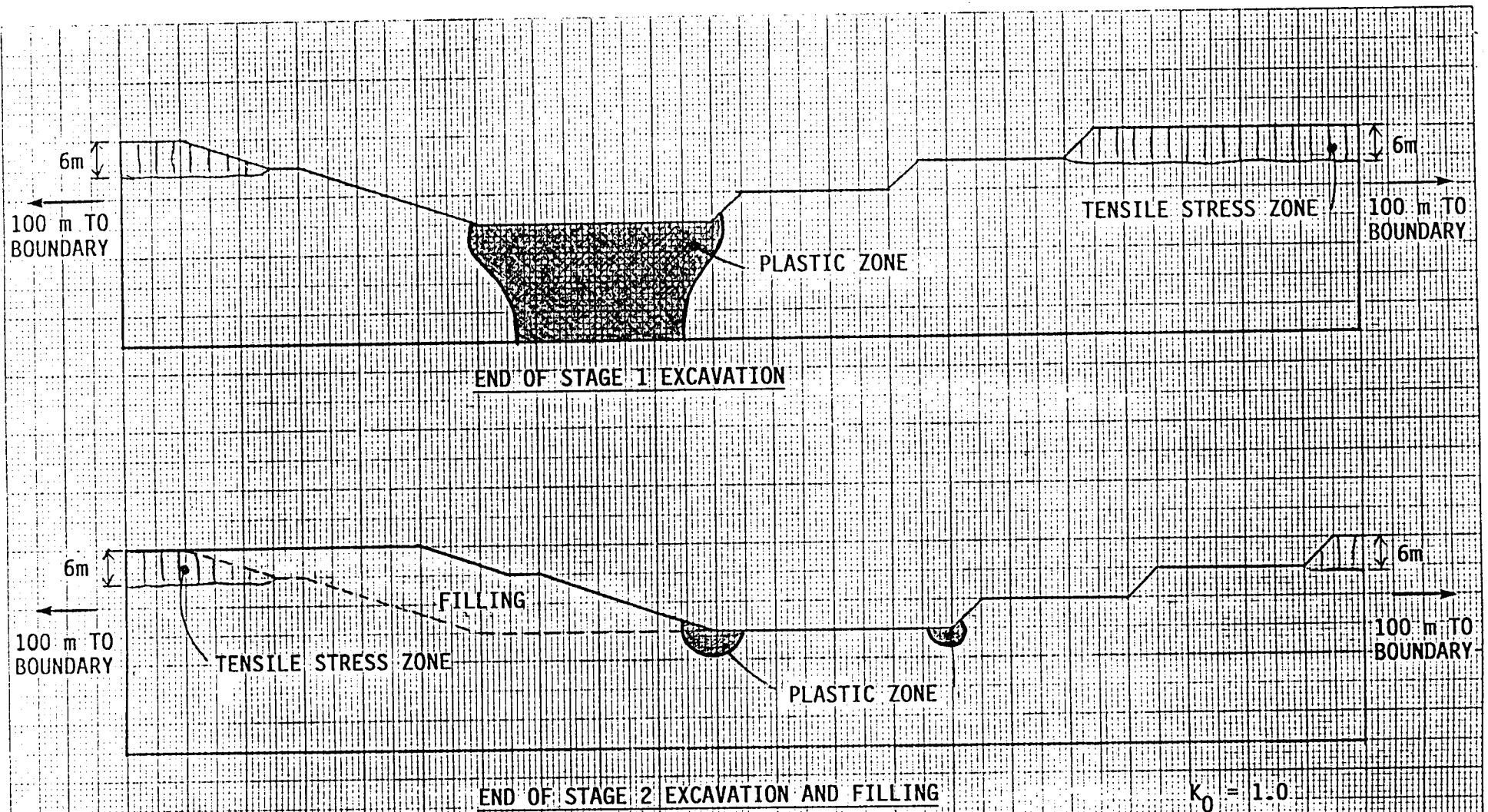
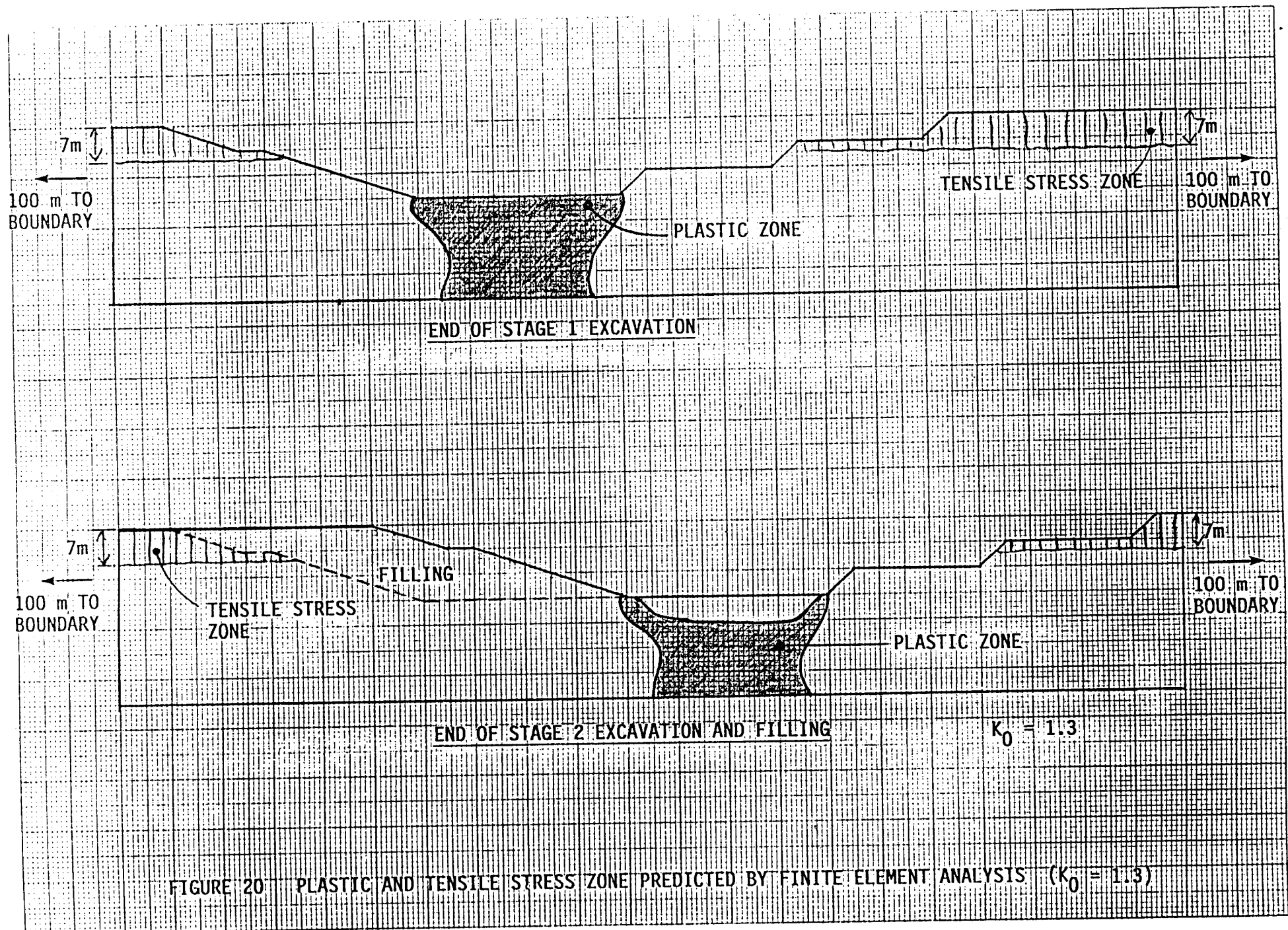


FIGURE 18 — PLASTIC AND TENSILE STRESS ZONE PREDICTED BY FINITE ELEMENT ANALYSIS ($K_0 = 0.7$)



$K_0 = 1.0$

FIGURE 19 PLASTIC AND TENSILE ZONE PREDICTED BY FINITE ELEMENT ANALYSIS ($K_0 = 1.0$)



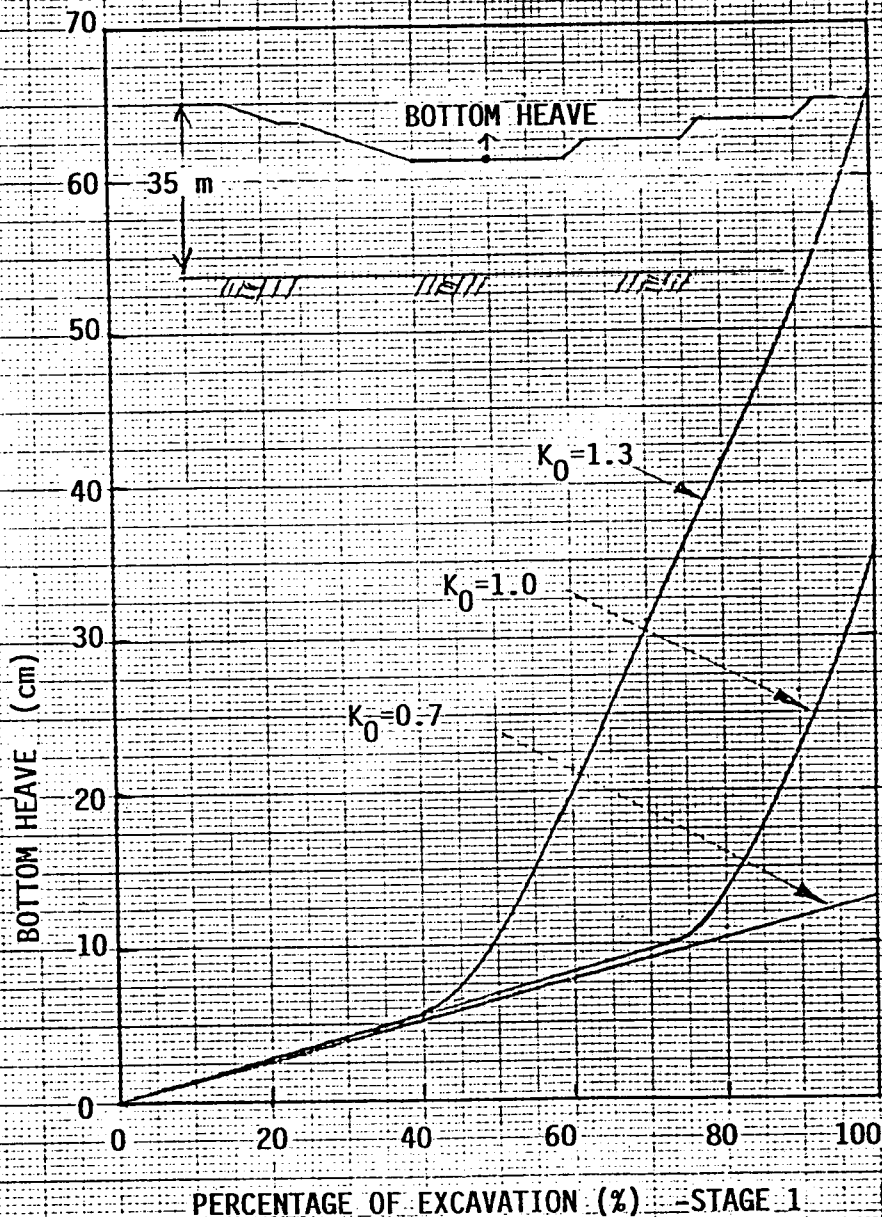


FIGURE 21 PREDICTED BOTTOM HEAVE VS. PERCENTAGE OF EXCAVATION

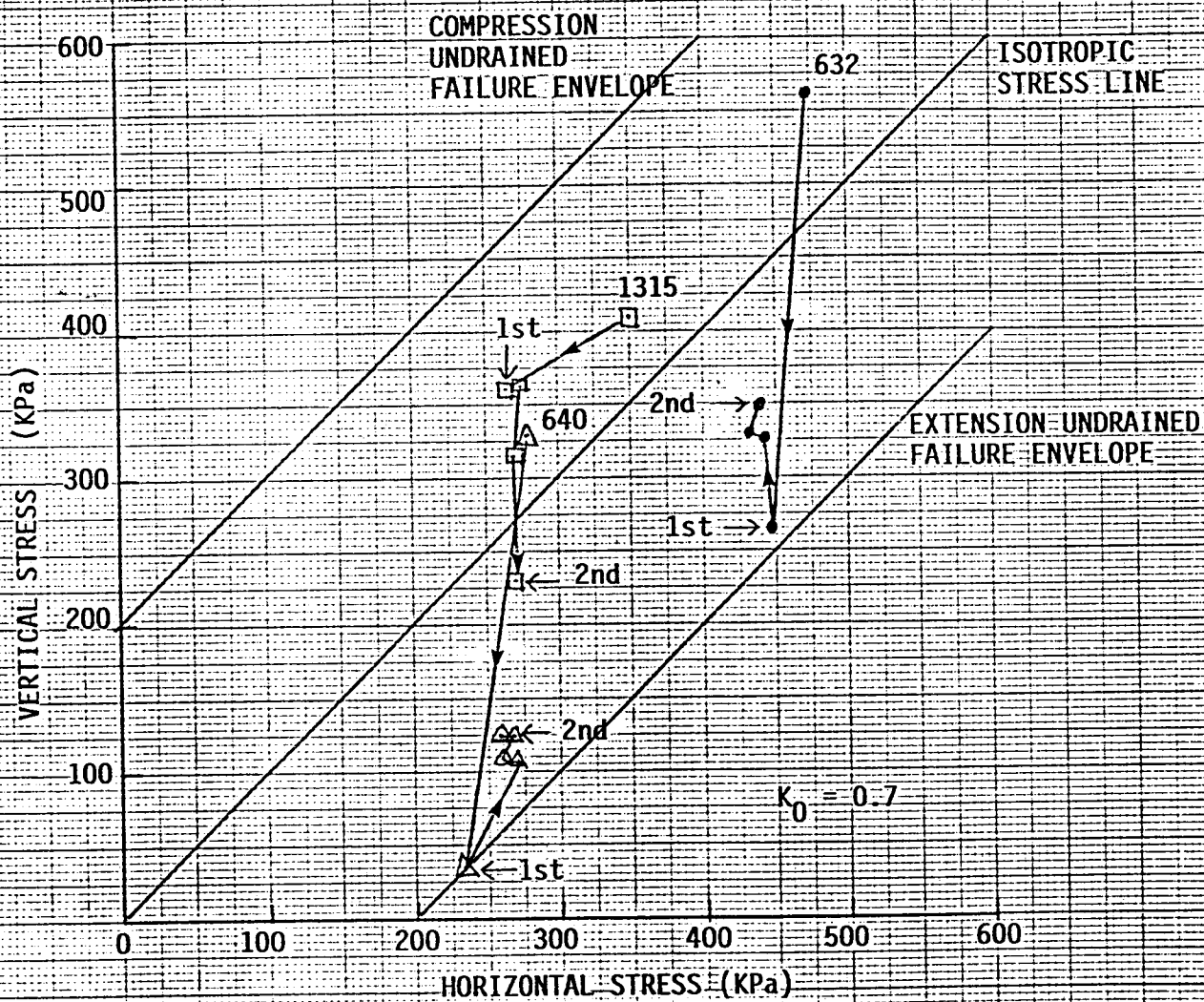


FIGURE 22 STRESS PATH PLOT FOR $K_0 = 0.7$

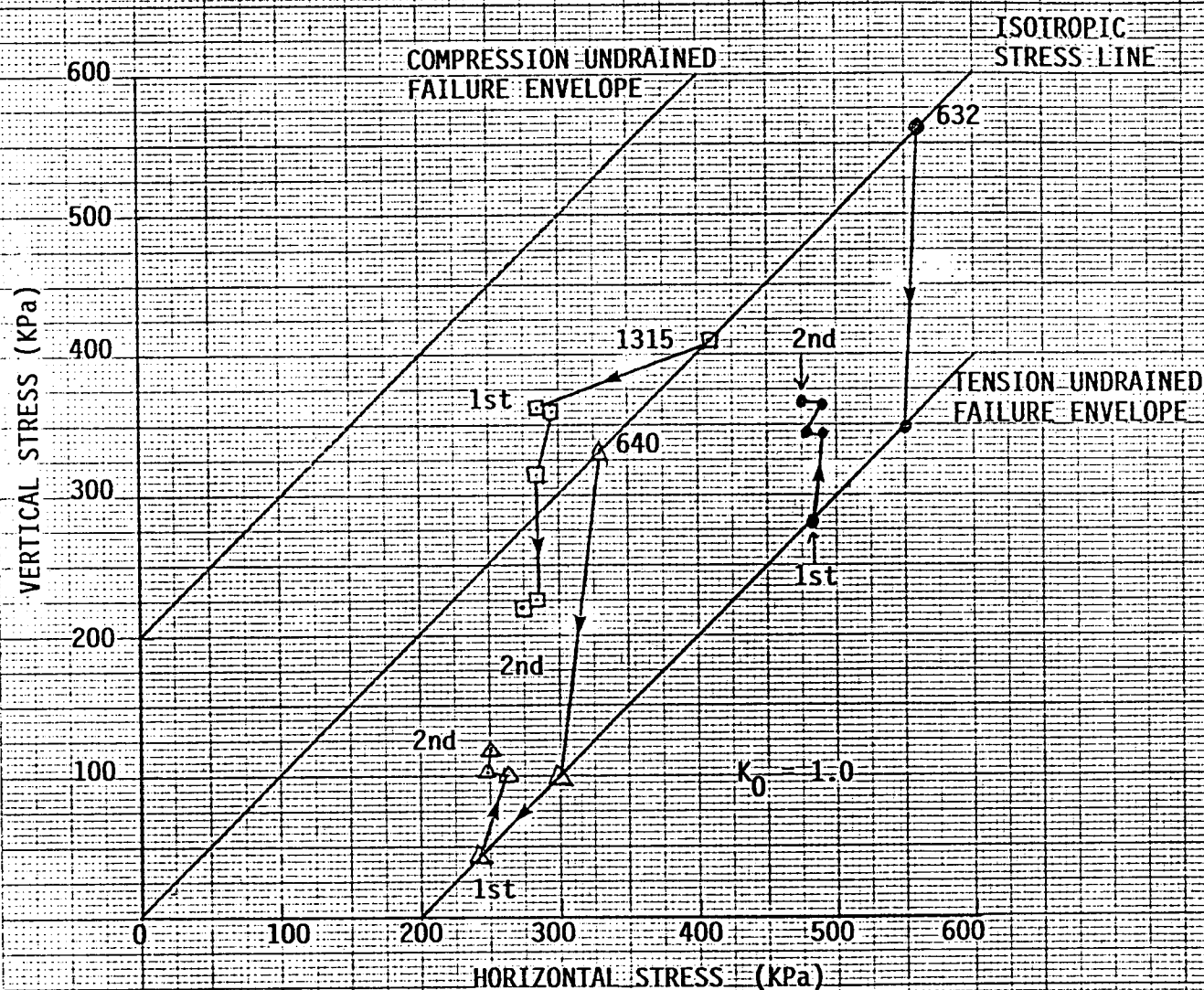


FIGURE 23 STRESS PATH PLOT FOR $K_0 = 1.0$

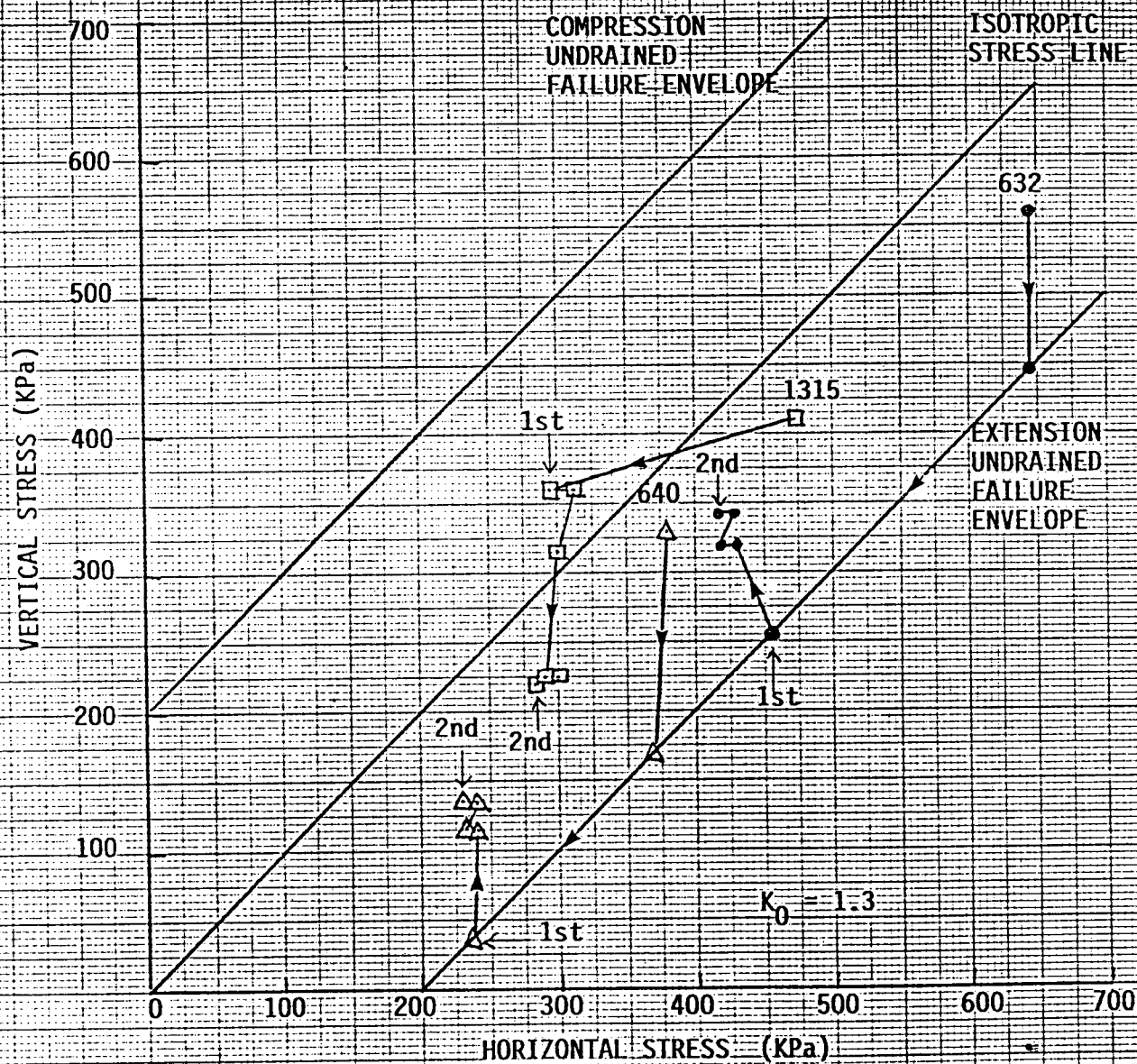


FIGURE 24 STRESS PATH PLOT FOR $K_0 = 1.3$

HORIZONTAL STRESS (KPa)

TENSION

COMPRESSION

-200

-100

0

100

200

$K_0 = 0.7$

DEPTH (m)

5

10

15

FIGURE 25: PREDICTED TENSILE STRESS DISTRIBUTION WITH DEPTH FOR $K_0 = 0.7$
AT LOCATION APPROXIMATELY 40m FROM THE CREST OF THE SIDESLOPES

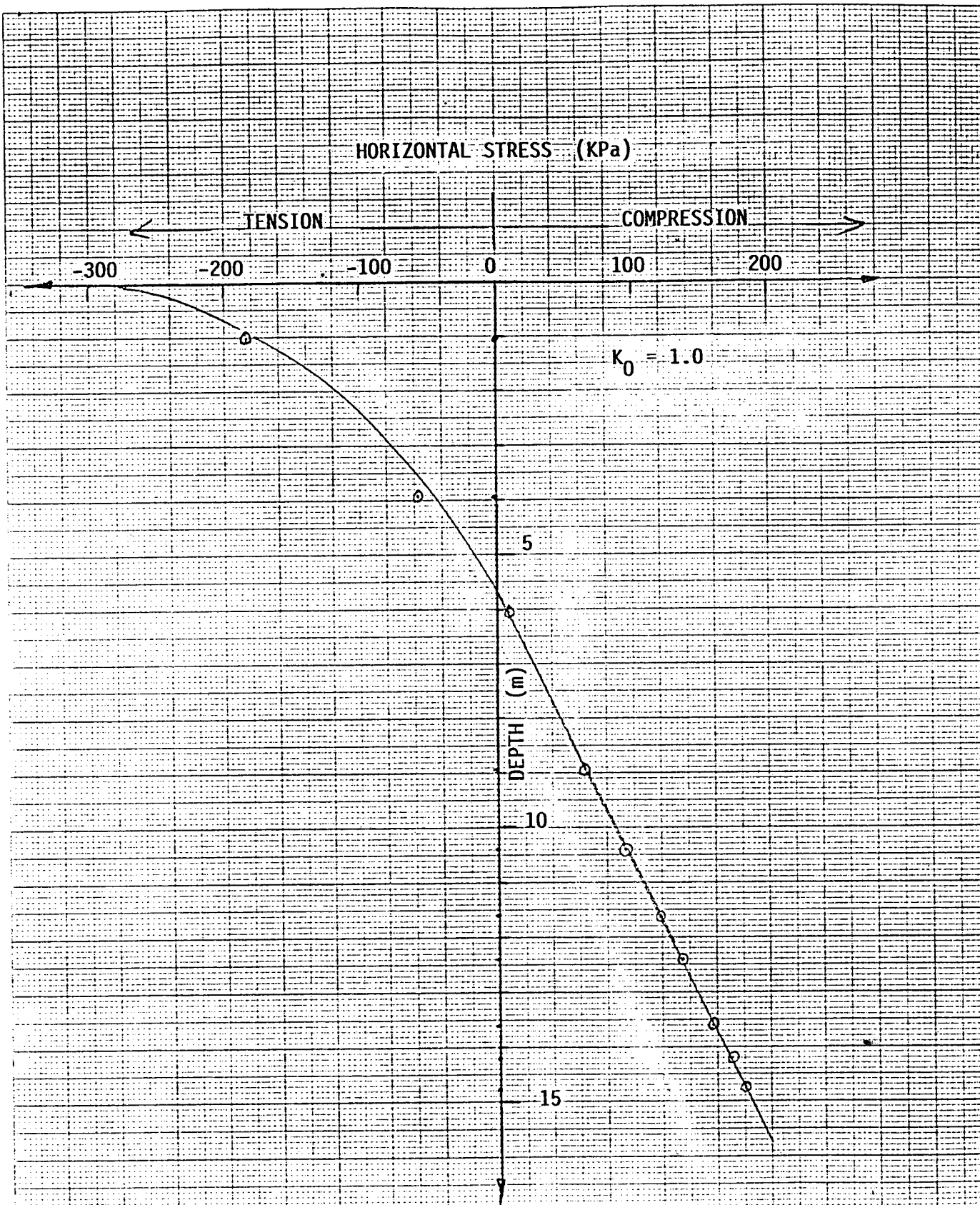


FIGURE 26 PREDICTED TENSILE STRESS DISTRIBUTION WITH DEPTH FOR $K_0 = 1.0$
AT LOCATION APPROXIMATELY 40m FROM THE CREST OF THE SIDESLOPES

HORIZONTAL STRESS (KPa)

TENSION

COMPRESSION

-300

-200

-100

0

100

200

$K_0 = 1.3$

DEPTH (m)

5

10

15

FIGURE 27 PREDICTED TENSILE STRESS DISTRIBUTION WITH DEPTH FOR $K_0 = 1.3$
AT LOCATION APPROXIMATELY 40m FROM THE CREST OF THE SIDESLOPES

APPENDIX I - FLANS (Finite Layer Analysis of Non-Homogeneous Soils)

INTRODUCTION - PURPOSE OF PROGRAM

Program FLANS (Version 4) is a computer program suitable for determining displacements (and some stresses) within an isotropic non-homogeneous elastic medium subjected to a uniform normal applied pressure.

The program FLANS has the following features:

- Circular (axi-symmetric), strip (plane strain) and rectangular (3D) loadings may be considered.
- Loading may be at the surface or beneath the surface.
- Soil/Rock layers may have a discrete variation in properties or a continuous (linear) variation in modulus with depth. (The program is currently dimensioned for upto 65 sublayers).
- The soil or rock deposit may have any depth, underlain by a rigid base, or may be infinite.
- Displacement (and some stresses) may be determined at user specified locations either on the loading plane or at points within the soil mass. (The program is currently dimensioned for upto 522 displacement determinations in one run).

This program is based on the finite layer theory proposed by Rowe and Booker (1982) which assumes that the elastic medium can be subdivided into distinct sub-layers in which the modulus varies exponentially with depth. The loading is then decomposed into Fourier Components and an analytic solution is found for each component. The final solution is obtained by synthesis of these solutions.

NUMERICAL APPROXIMATIONS AND INPUT CONSIDERATION

The method of analysis is essentially analytic in nature, however, two numerical approximations are required.

1. For input purposes, it is assumed that the soil modulus varies linearly with depth within a user defined layer; having a Youngs modulus E_i at the top of the layer i , an increase in Youngs modulus with depth ρ_i within layer i , and a constant Poisson's ratio ν_i .

For computational purposes the linear variation in modulus is approximated by an exponential function as indicated in Fig.A1. The accuracy of this approximation depends on the variation in modulus between the top and bottom of each layer. If this ratio is considered to be too large then each layer may be split into sublayers.

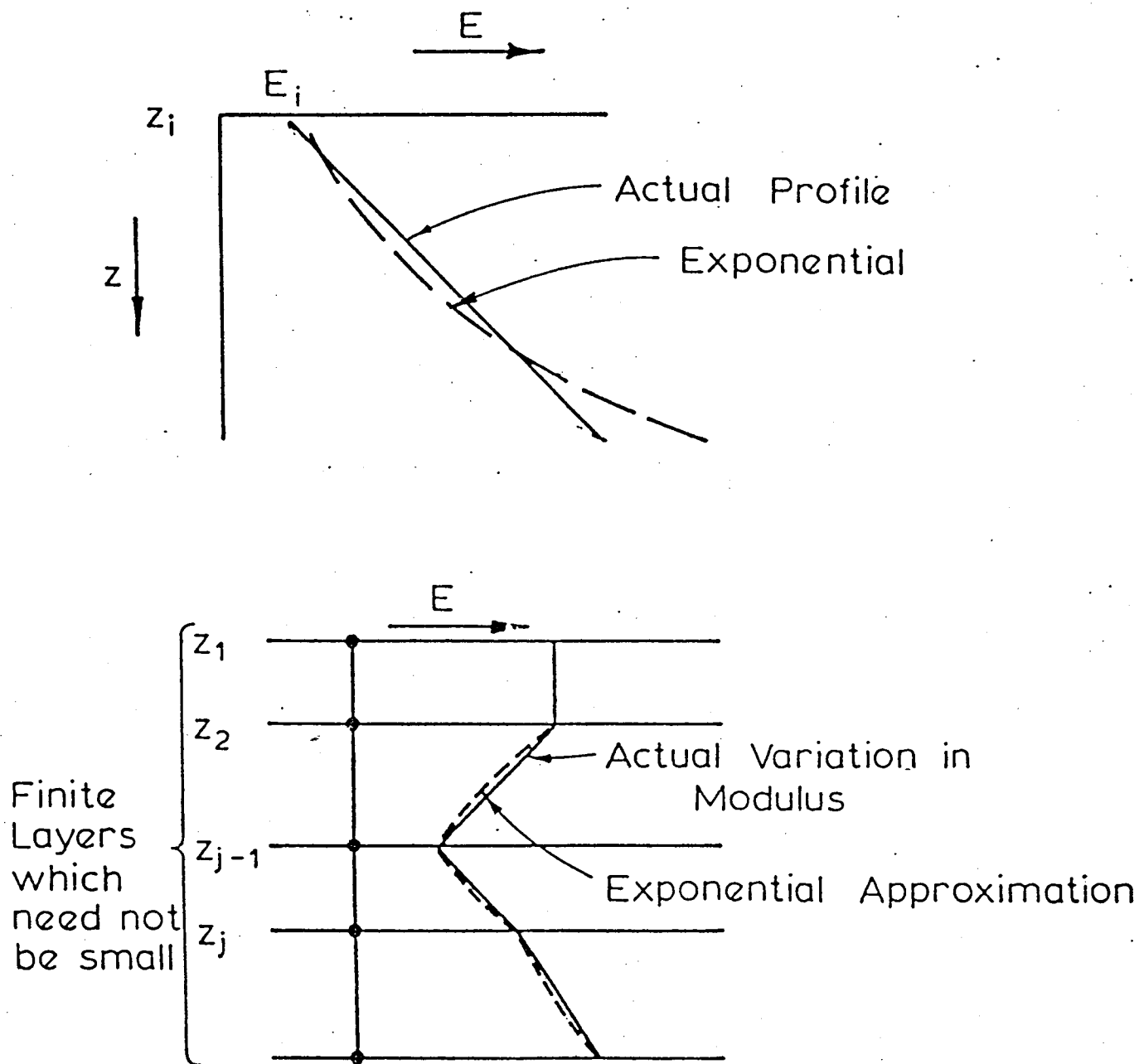


Figure A1

2. The theoretical development involves the use of a Fourier Transform and hence the synthesis of the final solution involves performing integrations of the form:

$$u_z(x,z) = \int_{-\infty}^{\infty} U_z(\alpha,z) e^{i\alpha x} d\alpha \quad \text{for plane strain} \quad (A1)$$

$$u_z(r,z) = \int_0^{\infty} 2\pi r J_0(\alpha r) U_z(\alpha,z) d\alpha \quad \text{for axi-symmetry} \quad (A2)$$

$$u_z(x,y,z) = \int_0^{\infty} \int_0^{2\pi} U_z(\alpha, \epsilon, z) e^{i\alpha (x \cos \epsilon + y \sin \epsilon)} d\epsilon d\alpha \quad \text{for full 3D conditions} \quad (A3)$$

These integrations are performed numerically by decomposing the integration range into a number of subintervals and then using Gauss quadrature within each subinterval. Thus, for example:

$$u = \int_0^{\infty} f(\alpha, r, z) d\alpha \approx \int_0^{n\Delta\alpha} f(\alpha, r, z) d\alpha \approx \sum_{j=1}^n \left(\sum_{k=1}^m f(\alpha_k, r, z) w_k \right) \quad (A4)$$

Where m is the number of sample points used for Gauss quadrature

n is the number of steps or subintervals

$\Delta\alpha$ is the width of each step or subinterval

Thus $n\Delta\alpha$ is the total width over which the integration is performed; and α_k and w_k represent the sample points and weighting functions corresponding to the level of Gauss quadrature to be used.

APPENDIX II - AFENA (AN ELASTIC-PLASTIC FINITE ELEMENT PROGRAM)

TITLE: A GENERAL FINITE ELEMENT ALGORITHM

PROGRAM: AFENA

MAINTENANCE: J.P. Carter, School of Civil and Mining Engineering, University of Sydney.
R.K. Rowe, Department of Civil Engineering, University of Western Ontario.

CAPABILITY: The program makes use of the finite element method of spatial discretisation for the numerical modelling of physical problems. A large library of element types is included for the solution of problems in 1, 2 and 3 spatial dimensions and in some cases the time domain. These element types allow the solution of problems in elastostatics, physical problems governed by the Laplace equation, statics of bodies of finite strength (elastoplastic problems), coupled problems such as consolidation and the dynamics of some elastic bodies.

Problem symmetry can be taken into account and a limited amount of mesh generation is included. Problems involving non-symmetric stiffness matrices may also be solved.

A special feature of this program is the ability to have the steps of any solution algorithm defined by the user. A set of macro instructions (or key words) is read from the main input file and the program then performs the tasks associated with these commands in the order of their appearance in the input data.

INPUT: Data describing the finite element mesh and material properties. Data describing the appropriate algorithm, i.e. a sequence of macro commands.

OUTPUT: Reformatted input data. Nodal variables, e.g. displacements, rotations, excess pore pressures etc. Integration point variables, e.g. stresses. Special purpose data, e.g. data for post-process mesh plotting and plotting of the nodal and Gauss point solutions.

METHOD: The finite element technique of spatial discretisation. Solution of the system of equations involves the use of a "skyline" technique. All mesh data, element and global matrices are stored in core. Large problems may thus require the use of a computer system with virtual memory.

LANGUAGE: ANSI FORTRAN77

PROGRAM AFENA

The program AFENA is an algorithm for the solution of boundary and initial value problems using the finite element techniques. It is a general finite element program in the sense that it may be used to obtain approximate solutions to problems in solid mechanics, particular problems in fluid mechanics, coupled problems, as well as other more general field problems. These may involve either one, two or three spatial dimensions as well as the time domain. Version 3.7 of the program has an element library containing twenty one different element types (see Table B1 for details); the emphasis is mainly on elements for the solution of deformation problems in continuum mechanics. However, the inclusion of additional elements into the library is relatively straightforward, although specific details for doing so are not given in this manual.

AFENA was developed from coding written by R.L. Taylor and published in Chapter 24 of 'The Finite Element Method' (3rd edition) by O.C. Zienkiewicz (McGraw-Hill, 1977). The original program has been much enlarged and enhanced but while AFENA now contains many additional features, it has retained the very versatile structure of Taylor's original program. Perhaps the most useful feature is the incorporation of a macro instruction language which can be used to construct specific algorithms, i.e. AFENA is basically a variable algorithm program. The user can create his own algorithm by specifying, in the appropriate order, a set of macro instructions selected from a list of possibilities. Each macro command acts as a signal to the program to carry out a predetermined sequence of computations.

In finite element analysis a system of linear equations in the nodal variables is developed. In AFENA these equations are solved using a "skyline" solution technique. The system of equations may be either non-symmetric or symmetric. In the latter case economies in storage and computation can be achieved by exploiting the symmetric nature of these equations. All mesh data, element and global matrices are stored in core; large problems may thus require the use of a virtual memory computer.

Element types are available in AFENA for the solution of one-, two- and three-dimensional problems in elastostatics, elastoplastic problems, physical problems governed by the Navier-Stokes equation, coupled problems such as Biot type consolidation and the dynamics of some elastic bodies. A list of element types in the library, together with brief details of each, is presented in Table B1.

In the present analysis, the soil was assumed to have an isotropic elastic-perfectly plastic constitutive relationship defined by two isotropic linear elastic parameters, an isotropic yield surface of Mohr-Coulomb type and an associated flow rule proposed by Davis (1968. Theories of plasticity and the failure of soil masses. Soil mechanics selected topics. Edited by I.K. Lee, Butterworths).

Table B1 Element Library

ELEMENT TYPE	BRIEF DESCRIPTION	GEOMETRY	SPECIAL CONDITIONS	STIFFNESS MATRIX
1	Linear isotropic elastic continuum	2-D	Plane strain or plane stress	Symmetric
2	Linear heat transfer (Laplace)	2-D	Axi-symmetric or Planar	Symmetric
3	Linear joint	2-D	Plane strain	Symmetric
4	Linear isotropic elastic continuum	2-D	Axi-symmetric	Symmetric
5	General linear elastic (9 constants) continuum	2-D	Plane strain	Non-symm.
6	Linear isotropic elastic continuum	2-D	Axi-symmetric geometry but non-symmetric loads and deformations	Symmetric
7	Linear elastic spring or spring or pin-ended bar	1-D	Planar problems	Symmetric
8	Linear elastic beam-column	1-D	Planar problems	Symmetric
9	Linear cross-anisotropic elastic continuum	2-D	Plane strain or plane stress	Symmetric
10	Not available
11	Linear isotropic elastic continuum	2-D	Axi-symmetric with initial strains	Symmetric
12-25	Not available

Table B1. Element Library (continued)

ELEMENT TYPE	BRIEF DESCRIPTION	GEOMETRY	SPECIAL CONDITIONS	STIFF MAT.
26	Fluid flow (non-linear and linear)	2-D	Planar flow	Non-symm. and symm.
27 *	Elastoplastic Mohr-Coulomb continuum	2-D	Plane strain	Non-symm. and symm.
28	Elastoplastic Mohr-Coulomb joint	2-D	Plane strain or axi-symmetric	Non-symm. and symm.
29	Non-linear spring or pin-ended bar	1-D	Planar problems	Symmetric
30	Linear isotropic elastic continuum	3-D	-	Symmetric
31	Elastoplastic Mohr-Coulomb continuum	2-D	Axi-symmetric	Non-symm. and symm.
32	Elastoplastic Mohr-Coulomb nodal joint	2-D	Planar problems	Non-symm. and symm.
33-50	Not available		
51	Biot consolidation. Linear isotropic skeleton, isotropic permeability	2-D	Plane strain	Symmetric
52	Biot consolidation. Linear isotropic skeleton, isotropic permeability	2-D	Axi-symmetric	Symmetric
53	Fully coupled, transient thermoelasticity	2-D	Plane strain	Symmetric
54	Biot consolidation. Linear isotropic skeleton isotropic permeability	2-D	Axi-symmetric geometry but non-symmetric loads and deformations	Symmetric

* Element type 27 - Elastoplastic element for plane strain condition was adopted in the present analysis. The material is linear, isotropic elastic until yield, which is determined by the Mohr-Coulomb criterion. Plastic flow is governed by either an associated or a non-associated flow rule.